

# The Global Determinants of International Equity Risk Premiums\*

Juan M. Londono<sup>†</sup>                      Nancy R. Xu<sup>‡</sup>  
Federal Reserve Board                  Boston College

February 14, 2023

## Abstract

We examine the commonalities in international equity risk premiums by linking *empirical evidence* for the ability of U.S. downside and upside variance risk premiums (DVP and UVP, respectively) to predict international stock returns with *implications* from an empirical model featuring asymmetric economic uncertainty and risk aversion. We find that DVP and UVP predict international stock returns through U.S. bad and good macroeconomic uncertainties, respectively. 60% to 80% of the dynamics of the global equity risk premium for horizons under seven months are driven by economic uncertainty, whereas risk aversion appears more relevant for longer horizons. The predictability patterns of DVP and UVP vary across countries depending on those countries' financial and economic exposure to global shocks. In those with higher economic exposure, investors demand higher compensation for bad macroeconomic uncertainty but lower compensation for good macroeconomic uncertainty, whereas the compensation for bad macroeconomic uncertainty is lower for countries with high financial exposure.

**JEL Classification:** F36, G12, G13, G15.

**Keywords:** variance risk premium, international stock return predictability, asymmetric state variables, cross-country variation in predictability

---

\*The views expressed in this document do not necessarily reflect those of the Federal Reserve System or its staff. We would like to thank Max Croce, Kasper Joergensen, Mete Kilic, Terry Pan, Frank Warnock, Dacheng Xiu, Guofu Zhou, Hao Zhou, and seminar/conference participants at the 2021 AEA meeting, the 2019 Stanford SITE, the 2019 NASMES Summer Meeting, the 2019 ECWFC at WFA, the 2019 EFA, the 2019 MFA, the 2019 FMA, the 2019 Global Conference in Latin America, the 2018 China International Risk Forum, the 2018 Econometric Society European winter meeting, and the Boston College (Carroll) and Boston Macro Juniors Workshop (MIT Sloan). The paper was previously circulated under the title "Variance Risk Premium Components and International Stock Return Predictability." All errors are our own.

<sup>†</sup>Division of International Finance, Federal Reserve Board, 20th Street and Constitution Avenue N.W., Washington, DC, 20551, U.S.; phone: 202-230-6938; email: juan.m.londono@frb.gov.

<sup>‡</sup>Boston College, Carroll School of Management, 140 Commonwealth Avenue, Chestnut Hill, MA, 02467, U.S.; phone: 617-552-2713; email: nancy.xu@bc.edu. Corresponding author.

# 1. Introduction

Contributing to extensive discussions on how global shocks transmit across international equity markets (see, e.g., Colacito, Croce, Gavazzoni, and Ready (2018)), we propose a new approach to examine which, and to what extent, common risk variables drive equity risk premiums (EPs) across countries at short (within one year) horizons. The main intuition of our analysis is that international stock return predictability should be driven by fundamental determinants that are common to global predictors and global EPs. By observing the predictability relations and the dynamics of global predictors, we can infer the relative importance of these common determinants in driving global equity risk compensations at various horizons.

In this paper, we formalize this intuition by linking novel *empirical evidence* for the ability of U.S. downside and upside variance risk premiums (DVPs and UVPs, respectively) to predict international stock returns with *implications* from an empirical model featuring time-varying and asymmetric (good and bad) U.S. economic uncertainty and risk aversion as common risk premium determinants. We find that 60% to 80% of the dynamics of the global EP for horizons under seven months are driven by economic uncertainty, while risk aversion appears more relevant for longer horizons. Both good and bad economic uncertainties contribute positively to the global EP, with the latter effect being more persistent and becoming dominant after four months. Our approach also allows us to systematically study the drivers of cross-country variations in global risk compensations. We find that in countries with higher economic exposure, investors demand higher compensation for bad economic uncertainty and lower compensation for good economic uncertainty; in countries with high financial exposure, they demand lower compensation for bad economic uncertainty.

For our empirical evidence, we consider the U.S. variance risk premium's (VP) downside and upside components as our two main global predictors, aiming to maximally infer information about short-horizon global equity risk compensations in light of the recent evidence in Kilic and Shaliastovich (2019) and Feunou, Jahan-Parvar, and Okou (2017). Our sample spans from April 1991 to December 2019. We calculate DVP and UVP as the difference between the risk-neutral and physical expectations of one-month-ahead stock return variance, conditional on whether the one-month-ahead stock price is below (bad states) or above (good states) the current stock price, respectively. We approximate the risk-neutral expectation of the downside (upside) stock return variance using puts (calls) on the S&P 500 index at different strikes and maturities. We obtain the physical expectation for the downside (upside) stock variation using the best forecast of the downside (upside) realized variance in a set of forecasting models. We find that DVP and UVP behave quite differently. In particular, the total VP and its downside component are highly correlated, significantly positive, and countercyclical, with large

positive spikes around key episodes of market stress and economic turmoil. In contrast, UVP is positive but smaller in magnitude, less persistent, and procyclical, with occasional negative spikes, some of which coincide with major positive DVP spikes.

We then document the predictive power of DVP and UVP for the excess returns of 22 countries' headline stock indexes expressed in U.S. dollars. We find evidence that decomposing the U.S. VP into its asymmetric components yields gains in predicting international stock returns. In addition, the predictability patterns of DVP and UVP are considerably different along several dimensions. In particular, the international stock return predictability is mainly explained by UVP at very short horizons and by DVP at horizons between four and seven months. Moreover, the predictive power of DVP follows a hump-shaped pattern, peaking at mid four- to seven-month horizons, while that of UVP follows a decreasing pattern after peaking at the one-month horizon.

There are variations in predictability patterns across countries, and we explore to what extent these variations are explained by country-level economic and financial exposure to global risks. Economic exposure is proxied by the ratio of a country's total international trade to its GDP, and financial exposure is proxied by the ratio of a country's total international asset and liability holdings to its GDP. We find that countries with higher economic (financial) exposure exhibit higher (lower) DVP coefficients, while the UVP coefficients significantly decrease with the economic exposure.

The second part of the paper formalizes the main intuition of our exercise using an empirical model wherein the VP components and international EPs are all linear functions of common risk premium determinants, and this function depends on current economic conditions. Our model can be motivated from a consumption-based asset-pricing framework where variance risk is priced. In such a framework, the dynamics of VP and international EPs should be driven by the second moments of kernel shocks, which we refer to as "common risk premium determinants." We assume that kernel disturbances come from asymmetric non-Gaussian shocks to the real growth process or the risk preference process. This assumption about the nature of kernel disturbances is consistent with extant findings that macroeconomic uncertainty and investors' attitudes toward risk play a prominent role in explaining the variance risk premium (including rare disasters in, e.g., Gabaix (2012); long-run risk models in, e.g., Bollerslev, Tauchen, and Zhou (2009); models with habit formation and bad environment-good environment dynamics, as in Bekaert and Engstrom (2017); and models with time-varying fear in, e.g., Drechsler (2013)). The global component of international EPs should reflect compensations for exposure to these kernel shocks. Intuitively, global shocks are capitalized in stock prices differently across countries as a result of heterogeneous exposure to these common shocks given a global representative investor. Because we observe the relation between VPs and international EPs through the predictability results, we can infer the relative importance of these common economic determinants in driving global equity risk compensations, which is the key

estimation strategy of the paper.

Bringing the empirical model to the data we find that, under normal economic cycle conditions, 62% of DVP variability is explained by risk aversion and 39% by bad economic uncertainty. Under volatile economic conditions, DVP becomes less sensitive to bad economic uncertainty, which is consistent with recent evidence on the time-varying disconnect between macro conditions and asset prices (see, e.g., Smith and Timmermann (2021) and Xu and You (2022)). UVP, on the other hand, increases with procyclical good economic uncertainty through the hedging demand of upside risk, as well as countercyclical risk aversion through the general hedging demand for variance risk. These two channels counteract, resulting in a relatively less persistent and smaller UVP than DVP.

We identify the relative importance of common economic determinants in international EPs by exploiting the cross section of country-level predictive coefficients. To characterize differences across countries, we consider measures of economic and financial exposure to global shocks, as motivated by our empirical evidence. We first make inferences for an average country, which is a country with a median level of economic and financial exposure. We find that the global EP's sensitivity to the common risk premium determinants changes over the horizon. Economic uncertainties explain 60% to 80% of the global risk premium variability at horizons under seven months, with bad uncertainty dominating after four months, while risk aversion has a stable and positive effect for all horizons. Both good and bad U.S. economic uncertainties contribute positively to the global EP, which is consistent with the domestic (U.S.) implications from Segal, Shaliastovich, and Yaron (2015).

We complement the analysis for the average country by calibrating four country groups with low and high economic and financial exposure. We find that global investors demand higher compensation for bad economic uncertainty (e.g., volatility caused by tail risk) and lower compensation for good economic uncertainty (e.g., volatility caused by growth spurts) in countries with higher economic exposure. Meanwhile, global investors demand lower compensation for bad economic uncertainty in countries with higher financial exposure; this finding is potentially consistent with the international risk sharing intuition, given lower cost of capital, greater firm and fundamental investment opportunities, and higher potential cash flow growth (e.g., Bekaert and Harvey (2003); Carrieri, Errunza, and Hogan (2007)).

## Related literature

Our research contributes to several strands of the literature. First, our exploration of the global determinants of international EPs contributes to the ongoing discussion of how global shocks matter and transmit across international equity markets (see, e.g., Colacito, Croce, Gavazzoni, and Ready (2018); Bonciani and Ricci (2020); Bekaert, Ho-

erova, and Xu (2020); Avdjiev, Gambacorta, Goldberg, and Schiaffi (2020); Aldasoro, Avdjiev, Borio, and Disyatat (2020); Xu (2019)). Unlike existing research, our framework exploits empirical evidence from international stock return predictability patterns, which allows us to look at global risk compensations using cross-sectional information at various horizons.

Our research joins the literature on understanding and estimating the dynamics of EPs, where researchers have used asset pricing models (as in Croce, Lettau, and Ludvigson (2015), Stathopoulos (2017), Martin (2017) and Bekaert, Engstrom, and Xu (2022)), surveys (as in Graham and Harvey (2005)), and novel data sets, such as dividend futures and dividend strips (as in Van Binsbergen, Brandt, and Koijen (2012) and Van Binsbergen, Hueskes, Koijen, and Vrugt (2013)). Our model estimation strategy features two innovations. First, in an asset pricing framework, both U.S. VP and international EPs should be driven by common risk premium state variables. Empirically, we observe their covariance relationship (i.e., predictability results) and the dynamics of the VP components. By predetermining the loadings of the VP components on these premium state variables, we can estimate the loadings of international EPs. Second, we are among the first to attempt incorporating multiple predictors and, in particular, multiple countries in a unified estimation framework.

Considering the U.S. VP and its asymmetric components as our main global predictors also contributes to the literature on international stock return predictability. Broadly, we add to a branch of the literature that investigates the predictive power of U.S. financial variables for international stock returns (see Rapach, Strauss, and Zhou (2013) and papers cited therein). More specifically, we add to the literature documenting the robust ability of the U.S. VP to predict international stock returns (Londono (2015) and Bollerslev, Marrone, Xu, and Zhou (2014)). A more recent strand of the VP predictability literature finds that compensations for bearing stock return variations associated with good and bad states are potentially different and that acknowledging asymmetry in the VP significantly increases its stock return predictability. This literature has focused only on VP's ability to predict U.S. stock returns (Kilic and Shaliastovich (2019), Feunou, Jahan-Parvar, and Okou (2017), and Feunou, Aliouchkin, Tédongap, and Xu (2020)). Given our goal to improve our understanding of global equity risk compensations through predictive coefficients, we contribute to this strand of the literature by showing that decomposing the U.S. VP into its downside and upside components also yields higher predictability for international stock returns.

Moreover, there is scant literature on the drivers of cross-country variation in predictability patterns. We explore the role of financial and economic exposure to global risks in explaining these variations. Importantly, our cross-country calibration suggests that global investors may demand more compensation for bad global economic uncertainty in countries with higher economic exposure but lower financial exposure, shedding

light on the non-trivial asset pricing implications of globalization (see, e.g., Kose, Prasad, Rogoff, and Wei (2009); Rapach, Strauss, and Zhou (2013); and Bekaert, Harvey, Kiguel, and Wang (2016)).

The remainder of the paper is organized as follows. Section 2 provides the empirical evidence for the dynamics and international stock return predictability of U.S. DVP and UVP. In Section 3, we introduce our empirical model and choices for the risk premium determinants. Section 4 presents the data and estimation methodology, and Section 5 discusses the main findings on the relative importance of these economic determinants in international EPs. Concluding remarks are included in Section 6.

## 2. Empirical Evidence

In this section, we explore the commonalities in short-term international EPs by examining the predictive power of the U.S. VP and its downside and upside components for international stock excess returns. In Sections 2.1 and 2.2, we construct and discuss the dynamic properties of the downside and upside components of the U.S. VP. We examine their predictive power for international stock excess returns and cross-country variations in international predictability patterns in Section 2.3. In Section 2.4, we construct global VP components and assess their predictive power to assess the robustness of our results using the U.S. VP components.

### 2.1. Definitions

We follow the notation in Bollerslev, Tauchen, and Zhou (2009) and define the total one-month-ahead VP as the difference between the risk-neutral ( $Q$ ) and the physical ( $P$ ) expectations of the total variance of one-month-ahead stock returns,

$$VP_{t,t+1} = V_t^Q(r_{t+1}) - V_t^P(r_{t+1}), \quad (1)$$

where  $r_{t+1}$  denotes the log stock return between months  $t$  and  $t + 1$ . We decompose VP into its downside and upside components, which we label DVP and UVP, respectively. These components allow us to disentangle the compensations for bearing downside and upside variance risks. The general expression for this decomposition is

$$VP_{t,t+1} = \underbrace{V_t^Q(r_{t+1}1_{<0}) - V_t^P(r_{t+1}1_{<0})}_{DVP} + \underbrace{V_t^Q(r_{t+1}1_{>0}) - V_t^P(r_{t+1}1_{>0})}_{UVP}, \quad (2)$$

where  $1_{<0}$  ( $1_{>0}$ ) is a dummy equal to 1 when the one-month-ahead return is below (above) 0 (see Feunou, Jahan-Parvar, and Okou (2017); Kilic and Shaliastovich (2019); and Held, Kapraun, Omachel, and Thimme (2020)).

We estimate the risk-neutral and physical components of DVP and UVP separately. The risk-neutral components of DVP and UVP are extracted from option prices (see, e.g., Britten-Jones and Neuberger (2000) and Andersen and Bondarenko (2009)) using

the option-implied downside and upside variances, respectively, as follows:

$$\begin{aligned} iv_{t,t+1}^D &= \left( \int_0^{S_t} \frac{2(1 + \log(S_t/K))}{K^2} P(t+1, K) dK \right)^2, \\ iv_{t,t+1}^U &= \left( \int_{S_t}^{\infty} \frac{2(1 - \log(K/S_t))}{K^2} C(t+1, K) dK \right)^2, \end{aligned} \quad (3)$$

where  $S_t$  is the current stock index price and  $P(K)$  ( $C(K)$ ) is the price of a put (call) with strike  $K$  and a one-month maturity. Intuitively, the option-implied downside (upside) variance is identified by put (call) options that pay off when the return realization is negative (positive). Next, we approximate the physical components of DVP and UVP using the expected values of one-month-ahead downside and upside realized variances, respectively. Intuitively, we separate the return variability due to intradaily negative and positive price movements, and the realized semivariances are obtained as follows:

$$\begin{aligned} rv_{t+1}^D &= \sum_{\tau=1}^N r_{\tau}^2 1_{r_{\tau} < 0}, \\ rv_{t+1}^U &= \sum_{\tau=1}^N r_{\tau}^2 1_{r_{\tau} > 0}, \end{aligned} \quad (4)$$

where  $r_{\tau}$  represents the instantaneous return calculated using stock prices sampled at intradaily frequencies between months  $t$  and  $t+1$  and  $N$  is the total number of high-frequency return observations within the month. The physical expectations of downside and upside realized variances are obtained using linear projections, as follows:

$$E_t(rv_{t+1}^i) = \hat{\alpha}^i + \hat{\gamma}^i \mathbf{G}_t^i, \quad (5)$$

where  $i = D$  (downside) or  $U$  (upside) and  $\mathbf{G}_t^i$  is a chosen set of predictors observable at time  $t$ . We allow  $\mathbf{G}_t^i$  to be different in predicting downside and upside realized variances and let the data decide the best predictive model for each VP component. Therefore, DVP and UVP are obtained, respectively, as follows:

$$\begin{aligned} vp_{t,t+1}^D &= iv_{t,t+1}^D - E_t(rv_{t+1}^D), \\ vp_{t,t+1}^U &= iv_{t,t+1}^U - E_t(rv_{t+1}^U). \end{aligned} \quad (6)$$

## 2.2. The dynamics of variance risk premiums

We use daily prices for options on the S&P 500 index at different strikes and maturities, sourced from OptionMetrics, to obtain the risk-neutral components of DVP and UVP, and we use intradaily S&P 500 index prices sampled every 15 minutes, sourced from Tickdata, to obtain the realized semivariances. Our sample period runs between April 1991 and December 2019.

While the literature has examined various models for predicting the total realized variance (see Bekaert and Hoerova (2014) for a thorough discussion), there is limited

research on predicting the downside and upside realized variances.<sup>1</sup> Table 1 explores five forecast specifications of one-month-ahead realized semivariances using the regression framework in Equation (5). The specification in measure (1) assumes that realized semivariances follow a Martingale process (see also Kilic and Shaliastovich (2019)), while measures (2) to (5) consider various combinations of predictors, including past realized variance and semivariances calculated at various horizons. Both the simple AR(1) and the heterogeneous autoregressive (HAR) framework using the past monthly ( $rv_{t-1m,t}^i$ ), weekly ( $rv_{t-5d,t}^i$ ), and daily ( $rv_{t-1d,t}^i$ ) realized semivariances significantly improve the goodness of fit for both downside and upside realized variances with respect to the Martingale specification.<sup>2</sup> In column (5), we include downside and upside option-implied variances, respectively. This last specification yields the best predictive performance for both downside and upside realized semivariances. Therefore, we use measure (5) to estimate the downside and upside expected physical variances.

With the risk-neutral and physical expected variance estimates, we obtain DVP and UVP as in Equation (6). The sum of the two VP components yields the total VP. In the remainder of the paper, we use the end-of-month estimates as our benchmark DVP and UVP measures.

We find that our benchmark monthly U.S. DVP and UVP measures differ in their unconditional and time-series properties. First, from Table 2, the option-implied downside variance is, on average, higher than the expected downside realized variance, which yields a positive DVP with an average of 15.97 squared percent. The positive nature of DVP holds for all other measures considered and is consistent with the evidence in the existing literature. DVP is prone to large positive realizations, including the large spike during the 2007-09 financial crisis, as shown in Figure 1. UVP is also, on average, significantly different from zero but considerably smaller than the average DVP (1.26 versus 15.97, respectively). As shown in Figure 1, UVP displays negative spikes in a few episodes. For instance, UVP reached negative 35.48 squared percent during the Lehman Brothers aftermath, which is almost 11 standard deviations away from its historical average.

Second, we find that the total U.S. VP comoves more closely to DVP than to UVP. Panel C of Table 2 shows that the correlation between VP and DVP using our chosen model is 0.97, while that between UVP and VP is 0.26. Moreover, our DVP and UVP measures are statistically uncorrelated. DVP and UVP are highly correlated across measures, with a correlation coefficient ranging from 0.74 to 0.99 for DVP and from 0.74

---

<sup>1</sup>Table A1 in the Internet Appendix shows the results of using alternative models to predict the total realized variance.

<sup>2</sup>This HAR framework for realized semivariances extends Corsi (2009), who focuses on forecasting the total realized variance. Feunou, Jahan-Parvar, and Okou (2017) also consider the HAR framework to approximate the expectations of downside and upside realized variances. However, they do not report the coefficients associated with the HAR components or the fit of the model, and they conclude that the results for the HAR specification are qualitatively similar to those for the Martingale specification.



to 0.95 for UVP (see Table A2 in the Internet Appendix.)

Third, the U.S. DVP exhibits a negative correlation with monthly U.S. industrial production growth ( $\rho = -0.29$ ); in contrast, UVP is positively correlated with the growth rate ( $\rho = 0.17$ ), suggesting weakly procyclical dynamics. Both correlations are statistically significant at the 1% level.

Fourth, the U.S. UVP is more transitory than DVP. The AR(1) coefficient of our DVP measure is 0.80, whereas that of our UVP measure is only 0.22. These four empirical facts are robust across alternative measures.

Taken together, our findings suggest that investors, in general, demand much higher compensation for downside shock exposure than for upside shock exposure, although, on average, investors dislike risks emanating from both tails. However, compensations demanded for bearing downside and upside variance risks have different dynamics in terms of their persistence and their relation with current economic conditions.

The properties of our U.S. VP measures are similar to those reported in the literature. For instance, Held, Kapraun, Omachel, and Thimme (2020) find that the U.S. DVP is, on average, positive and much larger in magnitude than UVP, and that UVP is also, on average, positive. In Kilic and Shaliastovich (2019), DVP is positive and UVP is, on average, negative (given our definition of VP, as they define VP as the difference between the physical and the risk-neutral expectations). Nevertheless, like ours, the UVP in Kilic and Shaliastovich (2019) remains positive most of the time except for a few sharply negative realizations. This difference is driven mostly by the fact that Kilic and Shaliastovich (2019) use the Martingale assumption when obtaining the physical expectation of the variance.<sup>3</sup>

## 2.3. International stock return predictability

We now examine the international stock return predictability patterns of U.S. DVP and UVP. We take the perspective of a global investor whose asset values are denominated in U.S. dollars. We consider the U.S. dollar excess returns of 22 countries' headline stock market indexes covering North America, Asia, and Europe. Log market returns are obtained from their total return indexes, sourced from DataStream, and the risk-free rate is the zero-coupon yield of U.S. Treasury bonds, sourced from Federal Reserve Economic Data (FRED). As before, our sample runs from April 1991 to December 2019 ( $T = 345$  months).

The main predictability regression is

$$\kappa^{-1}r_{t,t+\kappa}^i = a_\kappa + b_\kappa^D vp_{t,t+1}^D + b_\kappa^U vp_{t,t+1}^U + \epsilon_{i,t+\kappa}, \quad (7)$$

---

<sup>3</sup>Figure A1 in the Internet Appendix compares our benchmark VP measures with those obtained using the Martingale measure as in Kilic and Shaliastovich (2019). In unreported results, we show that the short-term predictability of UVP and DVP for international excess stock returns is robust to considering alternative VP measures, including the Martingale measure.

where  $t$  denotes the month and  $r_{t,t+\kappa}^i$  denotes the  $\kappa$ -month-ahead log excess returns for country  $i$ . A useful null regression specification imposes the same predictive coefficients for DVP and UVP. We control for country fixed effects to account for time-invariant characteristics.

Table 3 compares the results of the null and the main predictability regressions at the 1-, 3-, 6-, and 12-month horizons, and the full-horizon predictability patterns are shown in Figure A2 in the Internet Appendix. Our results for the null model are consistent with those in the literature (see, e.g., Londono (2015) and Bollerslev, Marrone, Xu, and Zhou (2014)). In particular, the hump-shaped predictability pattern of the total VP peaks at around the six-month horizon.

Our main empirical result is that acknowledging asymmetry in VP improves its predictability for international stock returns and therefore offers more joint information for understanding the latent behaviors of global EPs. The adjusted R-squareds of our main bivariate specification are larger than those of the null model for all within-one-year horizons considered.<sup>4</sup> In addition, the predictability patterns of DVP and UVP are different. While DVP exhibits a hump-shaped predictability pattern similar to that of total VP, UVP is a useful predictor mainly at short horizons. The variance decomposition (row “VARC%” in Table 3) confirms that the DVP contribution to predictability becomes dominant as the horizon increases, whereas the UVP contribution dominates mostly at horizons between one and three months. Our results thus suggest that decomposing the U.S. VP into its downside and upside components might introduce more flexibility in capturing the mixed underlying dynamics of international EPs at different horizons.

Next, we explore variations in DVP’s and UVP’s ability to predict stock returns across countries.<sup>5</sup> In a world economy with global agents and various sources of risk, cross-country differences in global risk compensations should intuitively be driven by their different risk exposures. We formalize this hypothesis and explore cross-country predictability variations, centering our attention on proxies for economic and financial exposure,  $EE^i$  and  $FE^i$ , respectively, as the main drivers. We propose the following

---

<sup>4</sup>The R-squareds for the null specification are considerably lower than those reported in Londono (2015) for two main reasons. First, our sample is longer (1991 to 2019 versus 1990 to 2012 in Londono (2015)). Second, our sample of international stock returns includes many more countries (22 versus 8). When we use the countries in our sample for the period between 1991 and 2012, R-squareds peak at 4% at the six-month horizon, which is closer to the results in Londono (2015) and to those in Bollerslev, Marrone, Xu, and Zhou (2014), using the global VP instead of the U.S. VP.

<sup>5</sup>Figures A3 and A4 in the Internet Appendix show the predictive coefficient estimates associated with DVP and UVP, respectively, in a country-level regression setting. In unreported results, which are available from the authors upon request, we show that the predictability patterns using our sample period and the country-level setting are robust to considering alternative VP measures, including Martingale measures, and to controlling for other predictors, including short-term interest rates, interest rate differentials, and stock valuation ratios.

setting:

$$\begin{aligned} \kappa^{-1}r_{t,t+\kappa}^i = & a_\kappa + (b_\kappa^D + b_{EE,\kappa}^D EE^i + b_{FE,\kappa}^D FE^i)vp_{t,t+1}^D \\ & + (b_\kappa^U + b_{EE,\kappa}^U EE^i + b_{FE,\kappa}^U FE^i)vp_{t,t+1}^U + \epsilon_{i,t+\kappa}. \end{aligned} \quad (8)$$

We use the time-series average of the trade-to-GDP ratio, sourced from the World Bank, to capture a country’s economic exposure (see, e.g., Alesina, Spolaore, and Wacziarg (2000) and de Soyres and Gaillard (2022)) and the time-series average of total foreign asset holdings from and to country  $i$  divided by its GDP to capture a country’s financial exposure (see, e.g., Schularick and Steger (2010)).<sup>6</sup> Table 4 presents the country-level exposure proxies (in percentages and as a proportion of the U.S. ratios) and classifies countries with relatively high (H), medium/average (M), and low (L) global exposure. The two exposure proxies are moderately correlated across countries ( $\rho=0.48$ ).

Table 5 shows the results for the setting in Equation (8). To facilitate the interpretation of our results,  $EE^i$  and  $FE^i$  are expressed as proportions to the U.S. ratios; that is, the financial and economic exposure of the United States is equal to 1. Thus, for each horizon, the coefficients  $b_\kappa^D + b_{EE,\kappa}^D + b_{FE,\kappa}^D$  and  $b_\kappa^U + b_{EE,\kappa}^U + b_{FE,\kappa}^U$  are the predictive coefficients of DVP and UVP, respectively, for U.S. stock excess returns. For most horizons,  $b_{EE,\kappa}^D$  ( $b_{FE,\kappa}^D$ ) is positive (negative) and significant, which suggests that higher economic (financial) exposure is associated with a higher (lower) DVP coefficient. The opposite relation is observed between UVP predictability and economic and financial exposure. In particular, for horizons of fewer than seven months,  $b_{EE,\kappa}^U$  ( $b_{FE,\kappa}^U$ ) is negative (positive) and significant (only for the two-month horizon).<sup>7</sup>

## 2.4. Global variance premium components

Thus far, we have considered the U.S. variance risk premium’s downside and upside components as our global predictors. Although DVP and UVP can also be calculated for other countries, data availability is limited to a handful of countries and for a much shorter sample than for the United States. To assess whether our results remain robust when we consider global predictors constructed using VPs from a collection of countries,

---

<sup>6</sup>Specifically, for country  $i$  in year  $t$ , we obtain the total asset holdings (equity and debt securities) of residents in country  $i$  in the rest of the world plus the total asset holdings of other countries’ residents in country  $i$ , and we divide this sum by country  $i$ ’s GDP; we then take the time-series average. The holding data are available at yearly frequency, and are obtained from Tables 1 and 8 from the Coordinated Portfolio Investment Survey conducted by the International Monetary Fund. The first available year is 2001.

<sup>7</sup>In Table A3 of the Internet Appendix, we show that our results remain robust if we consider a setting in which  $EE$  and  $FE$  are time varying. In Table A4, we also explore the robustness of our results to several alternative financial exposure measures: the ratio of international bank claims to GDP, sourced from the BIS, the capital market restriction index in Fernandez, Klein, Rebucci, Schindler, and Uribe (2016), and the equity market domestic investment share, sourced from the IMF’s CPIS. Our results remain robust for all variables except for a measure of domestic investment share, which is more closely related to home biasedness than financial exposure to global shocks. Overall, financial exposure seems to explain the cross-country predictability patterns mostly for horizons between 2 and 7 months for DVP.

we use the method described in Sections 2.1 and 2.2 to separately calculate DVPs and UVPs for Germany, France, and Switzerland for a sample starting in April 2003.<sup>8</sup> We also calculate a global average DVP and UVP as the equal-weighted averages of DVP and UVP for four countries (including the United States).

Table 6 shows a set of summary statistics for the international DVPs and UVPs and for their respective global averages. The main stylized facts documented for the U.S. DVP and UVP hold. In particular, for all countries and for their global average, it holds that (i) DVP is large and significant (panel A of Table 6) and displays positive spikes in episodes of heightened uncertainty; (ii) UVP is, on average, positive, quantitatively much smaller than DVP, and even statistically insignificant for Germany (panel B); and (iii) UVP displays large negative spikes, which often coincide with the positive DVP spikes.<sup>9</sup> Moreover, the variance premium components are highly correlated across countries, with correlations ranging between 0.85 and 0.93 for DVP (panel C) and between 0.72 and 0.87 for UVP (panel D). These high correlations imply that different weighting schemes used to calculate global averages should yield very similar results.

Table 7 compares the predictability patterns from the panel setting in Equation (7) using either the U.S. or the global averages of DVP and UVP for the overlapped sample starting in April 2003. Given the high correlation between the U.S. and the global average of the VP components (0.94 for DVP and 0.91 for UVP), it is not surprising that their predictability patterns are very similar. In particular, DVP predictability has a hump-shaped pattern that peaks at around the three- to six-month horizon, while the UVP predictability pattern is strictly decreasing. We relegate full-horizon predictability patterns to the Internet Appendix (see Figure A5).

Three main takeaways from this empirical section are important to the empirical model that we introduce next. First, U.S. DVP and UVP display different dynamics and are useful short-term predictors of international stock excess returns, which suggests distinct underlying determinants. Second, there are gains in acknowledging asymmetric risk compensations in international return predictability, which indicates the importance of asymmetric determinants. Third, there is some degree of cross-country variation in the predictability patterns and significance of the U.S. DVP and UVP driven by economic and financial exposure to global shocks, which suggests that there is information in the cross section that can be exploited to understand the global risk premium and the drivers

---

<sup>8</sup>To the best of our knowledge, the option data needed to calculate the VP components are only available for the following other countries: the Netherlands, the United Kingdom, and Japan. However, sufficient data to calculate the VP components for these countries start in the mid-2000s.

<sup>9</sup>Held, Kapraun, Omachel, and Thimme (2020) extend the calculation for the total VP and its components to eight international markets and their evidence is similar to ours. In particular, they find that DVP is, on average, consistently positive for all markets and much larger in magnitude than UVP. UVP is, on average, positive for the United States and France but turns negative for Germany and Switzerland.

of cross-country heterogeneity in global risk compensation.

### 3. An Empirical Model

In this section, we introduce an empirical model to understand the global determinants of international equity risk premiums by exploiting the ability of DVP and UVP to predict international stock returns documented in Section 2. The main intuition of the model is that the observed international stock return predictability should be driven by *common* economic determinants of VPs and short-term international EPs. Because we observe the relation between VPs and international EPs through the predictability results, we can infer the relative importance of these common economic determinants in driving global equity risk compensations across horizons. We introduce our empirical model and estimation strategy in Section 3.1 and our choices for the common determinants and their dynamics in Section 3.2.

#### 3.1. Estimation strategy

The main intuition for our estimation strategy comes from consumption-based frameworks that yield a variance risk premium. In particular, under certain kernel specifications (e.g., recursive preferences with long-run risk as in Bollerslev, Tauchen, and Zhou (2009), power utility with external habit formation and non-Gaussian shocks as in Bekaert and Engstrom (2017), or asymmetric jumps as in Kilic and Shaliastovich (2019)), variance risk is priced and its compensation is potentially asymmetric, given good or bad states of nature. The dynamics of VP and EP should both be driven by the second moments of kernel shocks. Extending this intuition to an international setting, assuming without loss of generality a global pricing kernel and comoving dividend growth processes, international EPs should reflect compensations for common exposures to these kernel shocks. In the rest of the paper, we refer to such second moments of kernel shocks as “common risk premium determinants.”

Given these economic intuitions, we propose an empirical model with a two-stage estimation strategy.<sup>10</sup> First, we denote our empirical proxies for DVP and UVP  $\widehat{vp}_t^D$  and  $\widehat{vp}_t^U$ , respectively, given the unknown loading parameter candidates, denoted by  $\mathbf{W}$ :

$$\begin{aligned}\widehat{vp}_t^D &= vp_0^D + (\mathbf{W}_0^{D'} + \mathbf{W}_1^{D'} z_t) \mathbf{X}_t, \\ \widehat{vp}_t^U &= vp_0^U + (\mathbf{W}_0^{U'} + \mathbf{W}_1^{U'} z_t) \mathbf{X}_t,\end{aligned}\tag{9}$$

where  $\mathbf{X}_t$  denotes a set of common risk premium state variables and  $\mathbf{W}_0^D$ ,  $\mathbf{W}_1^D$ ,  $\mathbf{W}_0^U$ , and  $\mathbf{W}_1^U$  are all constant matrices. We use the squared real growth innovation as a proxy for  $z_t$  to reflect potential risk premium nonlinearity in an uncertain economic environment (for reasons such as learning, as in David and Veronesi (2013), or arbitragers, as in

---

<sup>10</sup>Appendix B in the Internet Appendix introduces and solves a general, no-arbitrage international asset pricing model in closed-form that motivates our empirical model and choices.

Hong, Kubik, and Fishman (2012)). We estimate separate loadings of DVP and UVP on common risk premium state variables by jointly matching moments of the empirical estimates of DVP and UVP in a generalized method of moments (GMM) system.<sup>11</sup>

In the second stage, we write down the following general expression for country  $i$ 's equity risk premium for horizon (month)  $\kappa$ :

$$\widehat{EP}_{\kappa,t}^i = \left( \mathbf{V}'_{\kappa,0} + \mathbf{V}'_{\kappa,1} EE^i + \mathbf{V}'_{\kappa,2} FE^i + \mathbf{V}'_{\kappa,3} z_t \right) \mathbf{X}_t + \text{Idiosyncratic Part}, \quad (10)$$

where  $\mathbf{V}_{\kappa,0}$ ,  $\mathbf{V}_{\kappa,1}$ ,  $\mathbf{V}_{\kappa,2}$ , and  $\mathbf{V}_{\kappa,3}$  are all constant matrices that are common for all countries. To characterize heterogeneity in global compensations, we assume that the country-level loadings on common risk premium state variables are characterized by both economic and financial exposure to global risks, denoted  $EE^i$  and  $FE^i$ , respectively, and, as for VPs, by the squared real growth innovation. The modeling of cross-country heterogeneity is consistent with our empirical evidence (see Section 2.3), and can be motivated from an international asset pricing framework with comoving country dividend growth processes (see Internet Appendix B). The idiosyncratic part, which is not of interest for the purpose of our research, reflects compensations for country-specific risk factors that are orthogonal to the common risk component.

The model-implied  $\kappa$ -month predictive coefficients of DVP and UVP for country  $i$ 's EP can be then written as:

$$\begin{aligned} \widehat{b}_{\kappa}^{i,D} &\equiv \frac{\text{Cov}(\widehat{vp}_t^D, \widehat{EP}_{\kappa,t}^i)}{\text{Var}(\widehat{vp}_t^D)} = \frac{(\mathbf{V}_{\kappa}' \Xi \mathbf{W}^D)}{(\mathbf{W}^{D'} \Xi \mathbf{W}^D)}, \\ \widehat{b}_{\kappa}^{i,U} &\equiv \frac{\text{Cov}(\widehat{vp}_t^U, \widehat{EP}_{\kappa,t}^i)}{\text{Var}(\widehat{vp}_t^U)} = \frac{(\mathbf{V}_{\kappa}' \Xi \mathbf{W}^U)}{(\mathbf{W}^{U'} \Xi \mathbf{W}^U)}, \end{aligned} \quad (11)$$

where  $\mathbf{V}_{\kappa}^i$  denotes matrix  $\left[ \mathbf{V}'_{\kappa,0} + \mathbf{V}'_{\kappa,1} EE^i + \mathbf{V}'_{\kappa,2} FE^i \quad \mathbf{V}'_{\kappa,3} \right]'$ ;  $\Xi$  is the variance-covariance matrix of the risk premium determinants and of the risk premium determinants each multiplied by  $z_t$  (i.e., variance-covariance matrix of  $\left[ \mathbf{X}_t \quad \mathbf{X}_t z_t \right]'$ ).  $\mathbf{W}^D$ , which denotes matrix  $\left[ \mathbf{W}_0^{D'} \quad \mathbf{W}_1^{D'} \right]'$ , and  $\mathbf{W}^U$ , which denotes matrix  $\left[ \mathbf{W}_0^{U'} \quad \mathbf{W}_1^{U'} \right]'$ , are estimated from the first stage (Equation (9)).

In this second stage, we estimate unknowns in  $\{\mathbf{V}_{\kappa,0}, \mathbf{V}_{\kappa,1}, \mathbf{V}_{\kappa,2}, \mathbf{V}_{\kappa,3}\}$  one horizon at a time (for 12 horizons). For each horizon  $\kappa$ , the estimation is conducted by minimizing the sum of squared standardized distances between model-implied and empirical country-level predictive coefficients from Section 2.

<sup>11</sup>It may be quite natural to consider using simple ordinary least squares (OLS) projections to obtain these separate loadings. However, OLS regressions allow for residuals and do not guarantee dynamic moment matching; in addition, OLS regressions suffer from co-linearity given that, by design, our risk premium state variables comove with each other (e.g., risk aversion loads on growth shocks; see details in Section 3.2 and Internet Appendix C). Both concerns can be jointly resolved using a GMM framework.

### 3.2. Choices for common risk premium determinants

Our choices for common risk premium determinants,  $\mathbf{X}_t$  in Equations (9) and (10), are consistent with models in the consumption-based asset pricing literature that yield asymmetric variance risk compensations. Specifically, kernel disturbances come from asymmetric non-Gaussian shocks to the real growth process or from the risk preference process. As noted before, risk premium determinants should be second moments of kernel shocks.

We assume that the disturbances for the two fundamental state variables – real economic growth as denoted by  $\theta_t$  and relative risk aversion of the global representative agent as denoted by  $q_t$  – have the following joint dynamics (see Appendix C in the Internet Appendix for explicit expressions):

$$\begin{bmatrix} \theta_{t+1} - E_t(\theta_{t+1}) \\ q_{t+1} - E_t(q_{t+1}) \end{bmatrix} = \begin{bmatrix} \delta_{\theta,\theta p} & -\delta_{\theta,\theta n} & 0 & 0 \\ \delta_{q,\theta p} & \delta_{q,\theta n} & \delta_{q,qh} & -\delta_{q,ql} \end{bmatrix} \begin{bmatrix} \omega_{\theta p,t+1} \\ \omega_{\theta n,t+1} \\ \omega_{qh,t+1} \\ \omega_{ql,t+1} \end{bmatrix}, \quad (12)$$

where we assume flexible tail dynamics for the state variables. Specifically, as modeled in Bekaert, Engstrom, and Xu (2022), the disturbance of the real economic growth is decomposed into two independent centered gamma shocks:

$$\begin{aligned} \omega_{\theta p,t+1} &= \Gamma(\theta p_t, 1) - \theta p_t, \\ \omega_{\theta n,t+1} &= \Gamma(\theta n_t, 1) - \theta n_t. \end{aligned}$$

According to Equation (12), the total real growth disturbance is  $\delta_{\theta,\theta p}\omega_{\theta p,t+1} - \delta_{\theta,\theta n}\omega_{\theta n,t+1}$ . Given  $\delta_{\theta,\theta p}, \delta_{\theta,\theta n} > 0$  and the positive skewness of gamma distributions,  $\omega_{\theta p,t+1}$  ( $\omega_{\theta n,t+1}$ ) governs the right-tail (left-tail) dynamics of growth distribution with its time-varying shape parameter  $\theta p_t$  ( $\theta n_t$ ) determining the conditional higher moments of the growth disturbance shock. For example, given the moment generating function of independent gamma shocks, the conditional variance of  $\theta_{t+1}$  is  $\delta_{\theta,\theta p}^2 \theta p_t + \delta_{\theta,\theta n}^2 \theta n_t$  and the conditional unscaled skewness is  $2\delta_{\theta,\theta p}^3 \theta p_t - 2\delta_{\theta,\theta n}^3 \theta n_t$ . Increases in  $\theta p_t$  ( $\theta n_t$ ) imply higher (lower) conditional skewness while increasing conditional variance, and hence  $\theta p_t$  ( $\theta n_t$ ), can be interpreted as the “good” (“bad”) uncertainty state variable. This composite disturbance structure is one of the non-Gaussian shock assumptions that the literature has explored with the goal of modeling macro or financial state variable processes more realistically (see, e.g., Eraker and Shaliastovich (2008); Fulop, Li, and Yu (2015); Segal, Shaliastovich, and Yaron (2015); De Groot (2015); Bekaert and Engstrom (2017); and Xu (2021)). Similarly,  $\omega_{qh,t+1} \sim \Gamma(qh_t, 1) - qh_t$  and  $\omega_{ql,t+1} \sim \Gamma(\bar{q}l, 1) - \bar{q}l$  denote the high and low risk aversion shocks. We characterize the low risk aversion fluctuation as homoskedastic (i.e.,  $\bar{q}l$ ). This assumption aims to capture the possibility that most of the heteroskedasticity in risk aversion is driven by high risk aversion events, which helps keep the estimation

manageable.

Thus, there are four kernel shocks,  $[\omega_{\theta p,t+1}, \omega_{\theta n,t+1}, \omega_{qh,t+1}, \omega_{ql,t+1}]$ , which are mutually independent and follow centered gamma distributions with time-varying shape parameters, except, for simplicity, the low risk aversion fluctuation. We assume simple AR(1) processes for the good and bad economic uncertainty and the high risk aversion state variables; that is,  $\forall x_t \in \mathbf{X}_t \equiv [\theta p_t \ \theta n_t \ qh_t]$ ,

$$x_{t+1} = \mu_x + \rho_x x_t + \sigma_x \omega_{x,t+1}, \quad (13)$$

where all parameters are assumed to be positive and  $\mathbf{X}_t$  is the vector of risk premium determinants, given our non-Gaussian shock assumptions.

Analytically and statistically, Bekaert and Engstrom (2017) show that gamma shock assumptions are quite flexible in capturing realistic dynamics of fundamental higher moments while keeping the model tractable. Economically, this framework generates non-zero correlations between level and second (or higher-order) moment shocks, which is more consistent with existing empirical evidence (e.g., Adrian, Boyarchenko, and Giannone (2019) and Bekaert and Popov (2019)), while Gaussian-based frameworks typically separately model level and higher moment state variables. Equation (13) captures that when growth unexpectedly declines this period (i.e., a large realization of  $\omega_{\theta n,t} > 0$  in the left tail), one might expect a higher chance for extreme future growth declines, more growth volatility from the left tail, and more negative growth skewness (i.e., a higher  $\theta n_t$ ). Moreover, the conditional variance of the relative risk aversion state variable (inverse surplus consumption ratio) in Campbell and Cochrane (1999) also comoves positively with the relative risk aversion level, suggesting a potentially positive relationship between risk aversion level and volatility (see Xu (2021) for a detailed proof). The use of gamma shocks is suitable for our research because it efficiently summarizes conditional moments with one state variable, which allows us to realistically match the dynamics of variance and equity risk premiums while keeping the estimation system manageable in terms of the number of unknowns.

## 4. Data and Estimation

In this section, we estimate the parameters driving the dynamics of the common risk premium determinants and then estimate VP's and EP's loadings on these common risk premium determinants.

### 4.1. Risk premium determinants

We follow the empirical macro literature (e.g., Jurado, Ludvigson, and Ng (2015)) and use the change in the log U.S. industrial production (2007=100) as the empirical



proxy for real economic growth  $\theta_t$ . Time series for the U.S. industrial production index run from January 1947 to December 2019 and are obtained from FRED. We use the Approximate MLE methodology from Bates (2006) to estimate non-Gaussian fundamental shocks  $(\omega_{\theta p,t}, \omega_{\theta n,t})$  and uncertainty state variables  $(\theta p_t, \theta n_t)$ .

We then filter our risk aversion state variable and shocks from the risk aversion estimates provided by Bekaert, Engstrom, and Xu (2022).<sup>12</sup> Although measuring market-wide risk aversion is an ongoing debate, their measure is suitable for our research because it incorporates higher-order moment information from a wide range of financial and risk variables and focuses on identifying nonlinear patterns (e.g., monthly spikes).<sup>13</sup> The longest available sample for the Bekaert-Engstrom-Xu risk aversion measure starts in June 1986.

Table 8 shows summary statistics for the three time-varying risk premium determinants, and Figure 2 shows their estimated dynamics during our sample period. Detailed parameter estimates and long-sample time-series plots are available in Internet Appendix C. We discuss two observations that are relevant to our research. First, given the statistical properties of gamma distributions, when keeping the scale parameter fixed, a smaller shape parameter indicates that the distribution mass is more centered at the tail. Table 8 shows that the estimated good economic uncertainty state variable,  $\theta p_t$ , is, on average, higher than the estimated bad economic uncertainty state variable,  $\theta n_t$ , indicating that there is a higher chance of extreme values from the left tail of the real growth rate than from its right tail. Moreover,  $\theta p_t$  ( $\theta n_t$ ) is procyclical (countercyclical) given the significant negative (positive) correlation with the NBER recession indicator; intuitively, good (bad) economic uncertainty may spike during good (bad) economic conditions. According to the first two plots of Figure 2, both good and bad economic uncertainty state variables also appear quite persistent (with AR(1) coefficients of 0.972 and 0.911, respectively). While  $\theta p_t$  comoves mostly with major cyclical ups and downs,  $\theta n_t$  captures excessive left-tail events to industrial production, such as the effects of Hurricane Katrina (September 2005), the collapse of Lehman Brothers (October 2008), and the U.S.-China trade war (summer 2018). The bad uncertainty contributes, on average, 67% (and more during recessions) to the total conditional variance of economic growth.

Second, the risk aversion state variable  $qh_t$  captures the variability in the risk aversion shock that is cleansed from macroeconomic shocks. The estimated  $qh_t$  process is

---

<sup>12</sup>These authors provide both relative risk aversion ( $2\exp(q_t)$ ) and the risk aversion state variable ( $q_t = -s_t$ , where  $s_t$  is conceptually the log surplus consumption ratio as in a habit-formation model) on their websites. To precisely fit the purpose of our study, we use the time series of  $q_t$ .

<sup>13</sup>In comparison, the risk aversion measure of Campbell and Cochrane (1999) constructed as past quarterly consumption growth (Wachter (2006)) would not be suitable for our research because it is a “fundamental” variable (i.e., constructed from current and past quarterly or annual consumption growth). Miranda-Agrippino and Rey (2020) also provide a risk aversion measure, which is the residual of regressing their Global Financial Cycle series on current MSCI world realized return variance; their measure is also not suitable for our research because it uses price series observed from all geographical areas, while we focus on developed markets.

strictly countercyclical and positively skewed, exhibiting moderate monthly persistence. The time-series plot shows that risk aversion variability can also spike significantly in non-NBER recession episodes, such as the 1997 Asian Crisis, 9/11 and the corporate scandals during the 2000s, and the 2012 European Debt Crisis. We find that macroeconomic shocks account for about 15% of the total risk aversion variability.

## 4.2. Two-stage estimation and model fit

For the first-stage estimation of the GMM (Section 3.1), we use the empirical estimates of the VP components from Section 2 to generate orthogonality conditions: mean, variance, scaled skewness, scaled kurtosis of DVP and UVP (eight moments), the covariance between DVP and UVP (one), and the fraction of the DVP in total VP (one). Each raw moment condition is then tensor-multiplied with a set of lagged instruments  $\{1, \epsilon_{\theta,t-1}, \epsilon_{q,t-1}, \epsilon_{\theta,t-1}^2, \epsilon_{q,t-1}^2\}$ , where  $\epsilon_{\theta,t-1} = \theta_{t-1} - E_{t-2}(\theta_{t-1})$  and  $\epsilon_{q,t-1} = q_{t-1} - E_{t-2}(q_{t-1})$ . The GMM system has 50 moments and 14  $\mathbf{W}$  unknowns and is estimated iteratively. Then, for each horizon, the second-stage estimation takes the first-stage VP parameter estimates and the 44 international predictive coefficients (22  $\widehat{b}_{\kappa}^{i,D}$ 's and 22  $\widehat{b}_{\kappa}^{i,U}$ 's from the 22 countries) to obtain the 12  $\mathbf{V}$  unknowns from Equation (10) that determine the global risk compensation part of international EPs. We use a grid of 10,000 initial value combinations in each estimation.

Table 9 presents the moment-matching results and test specifications of the GMM system for the dynamics of the VP components. Unconditionally, all moments are significantly close to their empirical counterparts, and we fail to reject the Hansen's overidentification test. To evaluate the dynamic fit of DVP and UVP, Figure 3 shows that DVP and UVP estimates from the model (solid lines) are significantly correlated with their empirical counterparts (dashed lines) with coefficients of 0.85 and 0.47, respectively.

Table 10 illustrates the fit of the international predictive coefficient estimates of DVP and UVP by evaluating the fit of the model-implied mean, median, and standard deviation of the country predictive coefficients at each horizon. From panel A, the model fits the level and the cross-country dispersion of the DVP predictive coefficients quite well. Almost all model moments are within 1.645 standard deviations of the empirical counterparts; the only exception is the dispersion for the one- and two-month horizons. From panel B, both the model-implied level and cross-country dispersion of the UVP predictive coefficients are statistically close to their empirical counterparts, except for those beyond 10 months. These exceptions correspond to insignificant predictability coefficients from our empirical evidence. In general, our evidence suggests that the exposure measures, as conjectured in Equation (10), have the potential to explain the cross-country dispersion in the predictive coefficients.

Finally, we discuss three other observations from Table 10 that are consistent with

the empirical evidence. First, both the mean and the median of country predictive coefficients for the 22 countries are statistically close to the estimates in Table 3. Second, the model fit result also suggests that DVP and UVP should predict international EPs through different state variables, and the economic relevance of these state variables should be different across horizons. Third, the cross-country dispersion in DVP and UVP predictability also changes across horizons, suggesting that different international exposures may change both the level and the cross-horizon pattern of DVP or UVP predictability.

## 5. Economic interpretations

In this section, we discuss the economic interpretations of our empirical model. To obtain insight into both the dynamics of international EPs and the drivers of the transmission of VPs across countries, we use both the time-series return predictability and the variation in predictability across countries. As a result, through the lens of our model, we are able to interpret (i) the dynamics of the VP components; (ii) their stock return predictability in an “average” country with median economic and financial exposure levels, and (iii) their stock return predictability in countries with low or high economic and financial exposure levels. Taking these results together, we discuss the relationship between global determinants and international EPs across horizons, across time, and across countries.

### 5.1. The dynamics of the VP components

Table 11 presents the estimation results of the parameters from Equation (9) and the variance contribution (VARC) of each premium state variable. By construction, VARCs from the DVP system and the UVP system, respectively, should add up to 100%. From this table, DVP loads strongly and positively on variations in risk aversion that are not explained by business cycle fluctuations,  $qh_t$ . According to the variance decomposition results,  $qh_t$  accounts for 61.56% of the explained dynamics of DVP. The insignificant  $w_{qh,1}^D$  estimate indicates that DVP increases with risk aversion regardless of current business cycle conditions. In terms of economic magnitude, a one standard deviation (SD) increase in risk aversion is associated with a 0.77 SD increase in DVP. The bad economic uncertainty state variable,  $\theta_{n,t}$ , captures about 38.98% of the explained DVP dynamics during normal periods (i.e., when  $z_t$  is at its mean level). In addition, DVP loads less positively on bad uncertainty during periods of economic turmoil (i.e., when  $z_t$  is higher than its mean level), given the negative  $w_{\theta n,1}^D$  estimate; as a result, a one SD increase in bad uncertainty yields an increase in DVP that ranges between 0.55 and 0.62 SDs, depending on the state of the economy. This evidence is potentially consistent with

a widening disconnect between macro and asset prices under bad economic conditions due to, among other causes, structural breaks and policy expectations (see, e.g., Smith and Timmermann (2021) and Xu and You (2022)). Finally, the good economic uncertainty state variable,  $\theta p_t$ , has weaker statistical and economic significance in explaining DVP.

The evidence from Table 11 also suggests that UVP increases with *procyclical* good economic uncertainty, which can be explained through the hedging demand of upside volatility risk. In addition, UVP also increases with *countercyclical* bad economic uncertainty and risk aversion through the general risk compensation intuition. These counteracting drivers explain the relatively less persistent UVP dynamics, as documented in Section 2.2. UVP is, overall, statistically procyclical, which is consistent with the dominant positive contribution from the good economic uncertainty state variable. Interestingly, good economic uncertainty contributes slightly less positively to UVP during extremely volatile months, according to the negative  $w_{\theta p,1}^U$  estimate. One possible explanation is that economic fallout leads to less demand to hedge against future upside variance risk.

## 5.2. International stock return predictability: An average country view

We discuss the economic channels behind the ability of DVP and UVP to predict international stock returns for an “average” country with median financial and economic exposure to global shocks. We discuss the results using the mean value of  $z_t$ , as empirically  $z_t$  appears to play less of an economically important role in determining international EPs at the horizons of interests — the  $\mathbf{V}_{\kappa,3}$  coefficient estimates in Equation (10) are economically small.

Figure 4-(A) shows the model-implied effect of a one SD increase in a common risk premium state variable on an average country’s EP (in annualized percentages). For horizons up to seven months, where we center our attention, the three main common risk premium sources—good and bad economic uncertainties and risk aversion—contribute positively to the average country’s EP (or global EP), suggesting that the global investor demands, on average, positive compensations for individual countries’ exposure to global good and bad macro risk. Moreover, the sensitivity of global EPs to these state variables changes with the horizon. Economic risk compensation is crucial at short to mid horizons, which are also typically the horizons of interest for various dynamic equilibrium models in the literature. A one SD increase in bad economic uncertainty leads to an increase in the global EP of between 2 and 6 annualized percent, reaching peak impact around the three- to six-month horizons. This hump-shaped pattern (see the hollow dotted line) appears highly consistent with the DVP predictability pattern, as documented in Section 2. While both risk aversion and bad economic uncertainty meaningfully explain

the dynamics of DVP (see Section 5.1), this hump-shaped pattern suggests that DVP predicts international excess stock returns mainly through the bad economic uncertainty compensation channel. In contrast, good economic uncertainty is mainly relevant at very short horizons, which also matches with the UVP predictability pattern documented earlier.

As a result, through the lens of our estimation, both bad and good economic uncertainties play a significant role in explaining the EP of countries with median economic and financial exposure and their relative importance in explaining the variability of global EP change across horizons. Figure 4-(B) depicts the variance decomposition of the model-implied global equity risk compensation at various horizons and shows that economic uncertainties explain about 60% to 80% of the total variability at horizons under seven months.

Figure 5 depicts the time series of the model-implied international EP for an average country at several horizons of interest (all scaled to annualized percentages) and up to what extent this variation is explained by each state variable. Global EPs for these horizons generally comove closely and are countercyclical, which is consistent with the literature. Also, the global EP fluctuates less at longer horizons, such as 12 months. The shorter-term global EP appears to be particularly higher than its longer-term counterpart during periods of high economic uncertainty. For instance, during 1998 when good uncertainty spiked and during 2007 to 2008 when bad uncertainty spiked (see Figure 2), there are widening wedges between the shorter and the 12-month global EPs (see the second and third plots of Figure 5). This finding is consistent with Figure 4, where we show that economic uncertainties may be more important international EP determinants at shorter horizons, while risk aversion affects the whole term structure.

### **5.3. International stock return predictability: A cross-country view**

In this section, we complement our average country analysis and calibrate the results considering four country groups with low or high economic and financial exposure, where “low” (“high”) uses the 33rd (67th) percentile value of the exposure measures explained in Table 4.

Figure 6 is the cross-country version of Figure 4-(A), and the cross-country version of Figure 4-(B) is available in Internet Appendix C. First, if we compare the top two plots with the bottom two plots where economic exposure increases from low to high, we find that global investors demand higher bad economic uncertainty compensation as the hollow-dotted line moves upward. In contrast, good economic uncertainty compensation decreases as economic exposure increases. Thus, there appear to be two tales of increasing economic exposure. On the one hand, higher economic exposure means that it is harder to

diversify away “bad” global economic systemic risk, hence, the global investor demands higher compensation in such countries. On the other hand, higher economic exposure also implies that “good” global growth spurts could be transmitted to the economies of these countries, and while the good uncertainty compensation remains positive, it is smaller. Overall, these findings are consistent with the evidence in Table 5, where we document that countries with higher economic exposure exhibit a higher DVP coefficient (i.e., significant and positive  $b_{EE,\kappa}^D$ ) and a lower UVP coefficient (i.e., a significant and negative  $b_{EE,\kappa}^U$ ).

Comparing the left two plots with the right two plots where financial exposure increases from low to high, we can see that global investors demand lower bad economic uncertainty compensation as the hollow-dotted line moves downward. In other words, lower global bad macro risk compensation is demanded in countries with higher financial exposure. This result is consistent with the international financial openness literature, according to which global investors demand lower risk compensation given a lower cost of capital, greater firm and fundamental investment opportunities, and higher expected growth (e.g., Bekaert and Harvey (2003) and Carrieri, Errunza, and Hogan (2007)). Since financial exposure does not significantly explain the cross-country variation in the UVP predictive coefficient, as suggested by the insignificant coefficients  $b_{FE,\kappa}^U$  in Table 5, we focus on the determinants of DVP when discussing the effect of financial exposure.

To summarize, we find that global investors demand higher bad economic risk compensation in countries with higher economic exposure to global shocks and countries with lower financial exposure. It is noteworthy that, in the time series, risk aversion also explains the variability of DVP quite well. However, we find that DVP predicts international EPs and exhibits this particular hump-shaped predictability pattern through the bad economic uncertainty channel rather than through the risk aversion channel. This finding in turn suggests that economic uncertainties may be more important risk premium determinants at shorter horizons, while risk aversion could have a constant effect on the whole term structure. Hence, risk aversion appears less informative about the cross-country or cross-horizon patterns of international predictability that we document in this paper. While there is little research on upside or “good” variance risk compensation, we find that this is mostly determined by good economic uncertainty. In particular, countries with higher economic exposure exhibit a lower UVP coefficient, indicating that global investors demand lower good economic risk compensation.

## 6. Conclusion

Our understanding of the mechanisms behind the commonality in international equity premiums and the transmission of global risks across international financial markets remains an open debate in the literature. In this paper, we add to this debate using

a novel approach in which we link empirical evidence for the international stock return predictability of U.S. downside and upside variance risk premiums with the implications from an empirical model featuring asymmetric economic uncertainty and risk aversion using data for 22 countries from 1991 to 2019. We find that the international predictability patterns of DVP (positive and countercyclical) and UVP (smaller in magnitude and procyclical) are considerably different, with DVP being a robust mid-horizon (4-7 month) predictor and UVP a short-horizon (1-3 month) predictor. Moreover, predictive coefficient estimates vary across countries, and this variation can be well explained by each country's level of financial and economic exposure to global shocks. Then, through the lens of our empirical model, we find that DVP and UVP predict international stock returns through different common risk premium determinants, mainly bad and good U.S. macroeconomic uncertainties, respectively. Across countries, investors demand higher compensation for bad economic uncertainty and lower compensation for good economic uncertainty in countries with higher economic exposure, while they demand higher compensation for bad economic uncertainty in those countries with lower financial exposure.

Our approach of linking international predictability evidence with the implications from an empirical model allows us to use more information to infer the behavior of global risk compensations over time, across horizons, and across countries. This methodology should inspire several extensions of our work, including examining whether global risk premium determinants transmit through local currency equity risk pricing or through exchange rate channels, involving other international finance puzzles similar to the work in Colacito and Croce (2010) and Colacito, Croce, Gavazzoni, and Ready (2018). Moreover, our cross-country evidence should provide new testable hypotheses for future work on general equilibrium international models.

# References

- Adrian, T., Boyarchenko, N., Giannone, D., 2019. Vulnerable growth. *American Economic Review* 109, 1263–89.
- Aldasoro, I., Avdjiev, S., Borio, C. E., Disyatat, P., 2020. Global and domestic financial cycles: variations on a theme. *bis working paper no 864*.
- Alesina, A., Spolaore, E., Wacziarg, R., 2000. Economic integration and political disintegration. *American Economic Review* 90, 1276–1296.
- Andersen, T. G., Bondarenko, O., 2009. Dissecting the market pricing of return volatility. *working paper*.
- Avdjiev, S., Gambacorta, L., Goldberg, L. S., Schiaffi, S., 2020. The shifting drivers of global liquidity. *Journal of International Economics* 125, 103324.
- Bates, D. S., 2006. Maximum likelihood estimation of latent affine processes. *The Review of Financial Studies* 19, 909–965.
- Bekaert, G., Engstrom, E., 2017. Asset return dynamics under habits and bad environment–good environment fundamentals. *Journal of Political Economy* 125, 713–760.
- Bekaert, G., Engstrom, E., Xu, N. R., 2022. The time variation in risk appetite and uncertainty. *Management Science* 68, 3975–4004.
- Bekaert, G., Harvey, C. R., 2003. Emerging markets finance. *Journal of Empirical Finance* 10, 3–55.
- Bekaert, G., Harvey, C. R., Kiguel, A., Wang, X., 2016. Globalization and asset returns. *The annual review of financial economics* 8, 221–288.
- Bekaert, G., Hoerova, M., 2014. The vix, the variance premium and stock market volatility. *Journal of Econometrics* 183, 181–192.
- Bekaert, G., Hoerova, M., Xu, N. R., 2020. Risk, monetary policy and asset prices in a global world. *working paper*.
- Bekaert, G., Popov, A., 2019. On the link between the volatility and skewness of growth. *IMF Economic Review* 67, 746–790.
- Bollerslev, T., Marrone, J., Xu, L., Zhou, H., 2014. Stock return predictability and variance risk premia: statistical inference and international evidence. *Journal of Financial and Quantitative Analysis* 49, 633–661.
- Bollerslev, T., Tauchen, G., Zhou, H., 2009. Expected stock returns and variance risk premia. *The Review of Financial Studies* 22, 4463–4492.
- Bonciani, D., Ricci, M., 2020. The international effects of global financial uncertainty shocks. *Journal of International Money and Finance* 109, 102236.
- Britten-Jones, M., Neuberger, A., 2000. Option prices, implied price processes, and stochastic volatility. *The Journal of Finance* 55, 839–866.
- Campbell, J. Y., Cochrane, J. H., 1999. By force of habit: A consumption-based explanation of aggregate stock market behavior. *Journal of political Economy* 107, 205–251.
- Carrieri, F., Errunza, V., Hogan, K., 2007. Characterizing world market integration through time. *Journal of Financial and Quantitative Analysis* 42, 915–940.
- Colacito, R., Croce, M. M., 2010. The short and long run benefits of financial integration. *American Economic Review* 100, 527–31.



- Colacito, R., Croce, M. M., Gavazzoni, F., Ready, R., 2018. Currency risk factors in a recursive multi-country economy. *The Journal of Finance* 73, 2719–2756.
- Corsi, F., 2009. A simple approximate long-memory model of realized volatility. *Journal of Financial Econometrics* 7, 174–196.
- Croce, M. M., Lettau, M., Ludvigson, S. C., 2015. Investor information, long-run risk, and the term structure of equity. *The Review of Financial Studies* 28, 706–742.
- David, A., Veronesi, P., 2013. What ties return volatilities to price valuations and fundamentals? *Journal of Political Economy* 121, 682–746.
- De Groot, O., 2015. Solving asset pricing models with stochastic volatility. *Journal of Economic Dynamics and Control* 52, 308–321.
- de Soyres, F., Gaillard, A., 2022. Global trade and gdp comovement. *Journal of Economics, Dynamics, and Control* 138, 165–188.
- Drechsler, I., 2013. Uncertainty, time-varying fear, and asset prices. *The Journal of Finance* 68, 1843–1889.
- Eraker, B., Shaliastovich, I., 2008. An equilibrium guide to designing affine pricing models. *Mathematical Finance: An International Journal of Mathematics, Statistics and Financial Economics* 18, 519–543.
- Fernandez, A., Klein, M., Rebucci, A., Schindler, M., Uribe, M., 2016. Capital control measures: A new dataset. *IMF Economic Review* 64, 548–574.
- Feunou, B., Aliouchkin, R. L., Tédongap, R., Xu, L., 2020. The term structures of expected loss and gain uncertainty. *Journal of Financial Econometrics* 18, 473–501.
- Feunou, B., Jahan-Parvar, M. R., Okou, C., 2017. Downside variance risk premium. *Journal of Financial Econometrics* 16, 341–383.
- Fulop, A., Li, J., Yu, J., 2015. Self-exciting jumps, learning, and asset pricing implications. *The Review of Financial Studies* 28, 876–912.
- Gabaix, X., 2012. Rare disasters: An exactly solved framework for ten puzzles in macro-finance. *The Quarterly Journal of Economics* 127, 645–700.
- Graham, J. R., Harvey, C. R., 2005. The long-run equity risk premium. *Finance Research Letters* 2, 185–194.
- Held, M., Kapraun, J., Omachel, M., Thimme, J., 2020. Up-and downside variance risk premia in global equity markets. *Journal of Banking and Finance* 118.
- Hong, H., Kubik, J. D., Fishman, T., 2012. Do arbitrageurs amplify economic shocks? *Journal of Financial Economics* 103, 454–470.
- Jurado, K., Ludvigson, S. C., Ng, S., 2015. Measuring uncertainty. *American Economic Review* 105, 1177–1216.
- Kilic, M., Shaliastovich, I., 2019. Good and bad variance premia and expected returns. *Management Science* 65, 2445–2945.
- Kose, M. A., Prasad, E., Rogoff, K., Wei, S.-J., 2009. Financial globalization: a reappraisal. *IMF Staff papers* 56, 8–62.
- Londono, J. M., 2015. The variance risk premium around the world. working paper.
- Martin, I., 2017. What is the expected return on the market? *The Quarterly Journal of Economics* 132, 367–433.

- Miranda-Agrippino, S., Rey, H., 2020. Us monetary policy and the global financial cycle. *The Review of Economic Studies* 6, 2754–2776.
- Rapach, D. E., Strauss, J. K., Zhou, G., 2013. International stock return predictability: what is the role of the united states? *The Journal of Finance* 68, 1633–1662.
- Schularick, M., Steger, T. M., 2010. Financial integration, investment, and economic growth: evidence from two eras of financial globalization. *The Review of Economics and Statistics* 92, 756–768.
- Segal, G., Shaliastovich, I., Yaron, A., 2015. Good and bad uncertainty: Macroeconomic and financial market implications. *Journal of Financial Economics* 117, 369–397.
- Smith, S. C., Timmermann, A., 2021. Break risk. *The Review of Financial Studies* 34, 2045–2100.
- Stathopoulos, A., 2017. Asset prices and risk sharing in open economies. *The Review of Financial Studies* 30, 363–415.
- Van Binsbergen, J., Brandt, M., Koijen, R., 2012. On the timing and pricing of dividends. *American Economic Review* 102, 1596–1618.
- Van Binsbergen, J., Hueskes, W., Koijen, R., Vrugt, E., 2013. Equity yields. *Journal of Financial Economics* 110, 503–519.
- Wachter, J. A., 2006. A consumption-based model of the term structure of interest rates. *Journal of Financial economics* 79, 365–399.
- Xu, N. R., 2019. Global risk aversion and international return comovements. working paper.
- Xu, N. R., 2021. Procyclicality of the comovement between dividend growth and consumption growth. *Journal of Financial Economics* 139, 288–312.
- Xu, N. R., You, Y., 2022. Main street’s pain, wall street’s gain. working paper.

Table 1: Expected downside and upside realized variances

This table shows the coefficients associated with the predictors of one-month-ahead (22 days) downside and upside realized variances in panels A and B, respectively. The specification in column (1) assumes that realized variances follow a Martingale ( $E(rv_{t+1}^i) = rv_t^i$ , for  $i = D, U$  (downside or upside)). For the specifications in columns (2) to (5), we estimate the following regression setting:

$$E_t(rv_{t+1m}^i) = \hat{\alpha}^i + \hat{\gamma}^i \mathbf{G}_t^i.$$

We consider the following predictors,  $\mathbf{G}_t$ , at time  $t$ : the total realized variance calculated over the last month ( $rv_{t-1m,t}$ ) and its downside and upside components ( $rv_{t-1m,t}^i$ ); realized semivariances calculated using either the last five days ( $rv_{t-5d,t}^i$ ) or the last day of the month ( $rv_{t-1d,t}^i$ ); and the downside and upside components of the option-implied variance ( $iv_{t,t+1m}^i$ ). All regressions are estimated using daily data. The sample runs from April 1991 to December 2019. Heteroskedasticity and autocorrelation consistent (HAC) standard deviations with 44 lags are reported in parentheses. \*\*\*, \*\*, and \* represent significance at the 1%, 5%, and 10% confidence levels. The adjusted  $R^2$ s are reported at the end of each panel.

	(1)	(2)	(3)	(4)	(5)
Panel A. Downside realized variance					
Constant	0	4.17***	4.11***	3.88***	3.18***
	-	(0.63)	(0.67)	(0.55)	(1.00)
$rv_{t-1m,t}$			0.43 (0.36)		
$rv_{t-1m,t}^D$	1	0.62***	0.10	0.29**	0.23***
		(0.07)	(0.21)	(0.13)	(0.08)
$rv_{t-5d,t}^D$				0.29**	0.27*
				(0.13)	(0.15)
$rv_{t-1d,t}^D$				0.06***	0.04*
				(0.01)	(0.03)
$iv_{t,t+1m}^D$					0.08 (0.10)
Adj. $R^2$	0.230	0.378	0.378	0.428	0.429
Panel B. Upside realized variance					
Constant	0	3.73***	3.80***	3.39***	0.84
	-	(0.64)	(0.64)	(0.59)	(0.73)
$rv_{t-1m,t}$			-0.60 (0.40)		
$rv_{t-1m,t}^U$	1	0.64***	0.61***	0.30**	0.07
		(0.08)	(0.17)	(0.15)	(0.11)
$rv_{t-5d,t}^U$				0.30**	0.24
				(0.15)	(0.15)
$rv_{t-1d,t}^U$				0.05***	0.03**
				(0.01)	(0.01)
$iv_{t,t+1m}^U$					0.57*** (0.11)
Adj. $R^2$	0.290	0.414	0.433	0.461	0.499

Table 2: Summary statistics for variance premium components

This table reports time-series averages of the monthly risk-neutral and physical expectations of the variances ( $iv_{t,t+1}$  and  $E_t(rv_{t,t+1})$ , respectively) as well as the corresponding monthly variance premiums (VPs). The monthly time series are end-of-month estimates from Table 1. All measures are in units of monthly variance—i.e., in annual percentage squared divided by 12 (as commonly used in the literature; see, e.g., Bekaert and Hoerova (2014) and Kilic and Shaliastovich (2019)). For VP estimates, we also report standard deviations and minimum and maximum values. The sample runs from April 1991 to December 2019.

	(1)	(2)	(3)	(4)	(5)
Panel A. DVP					
$Mean(iv_{t,t+1}^D)$	23.67	23.67	23.67	23.67	23.67
$Mean(E_t(rv_{t,t+1}^D))$	10.87	7.04	7.08	7.05	7.69
$Mean(vp_{t,t+1}^D)$	12.79	16.63	16.58	16.61	15.97
$SD(vp_{t,t+1}^D)$	11.24	14.08	14.10	13.85	13.52
$Min(vp_{t,t+1}^D)$	-23.49	2.47	2.41	2.21	2.24
$Max(vp_{t,t+1}^D)$	81.25	97.91	99.64	91.00	93.05
Panel B. UVP					
$Mean(iv_{t,t+1}^U)$	11.03	11.03	11.03	11.03	11.03
$Mean(E_t(rv_{t,t+1}^U))$	10.50	7.07	7.02	7.34	9.76
$Mean(vp_{t,t+1}^U)$	0.53	3.96	4.01	3.69	1.26
$SD(vp_{t,t+1}^U)$	9.76	6.19	6.15	6.30	3.28
$Min(vp_{t,t+1}^U)$	-138.25	-59.87	-64.41	-62.93	-35.48
$Max(vp_{t,t+1}^U)$	23.27	31.07	22.70	26.17	9.56
Panel C. Correlations within models					
$Correl(vp_{t,t+1}^D, vp_{t,t+1}^D)$	0.85	0.95	0.94	0.93	0.97
$Correl(vp_{t,t+1}^D, vp_{t,t+1}^U)$	0.79	0.69	0.65	0.59	0.26
$Correl(vp_{t,t+1}^U, vp_{t,t+1}^D)$	0.35	0.43	0.36	0.25	0.03

Table 3: International predictability of VP and its components

This table reports evidence for the ability of the variance premium and its components to predict international stock returns at various horizons of interest (in units of months). Our main specification is the following:

$$\kappa^{-1}r_{t,t+\kappa}^i = a_\kappa + b_\kappa^D vp_{t,t+1}^D + b_\kappa^U vp_{t,t+1}^U + \epsilon_{i,t+\kappa},$$

where  $r_{t,t+\kappa}^i$  denotes the  $\kappa$ -month-ahead log excess returns for country  $i$  and  $vp_{t,t+1}^D$  and  $vp_{t,t+1}^U$  denote downside and upside variance premium (DVP and UVP) estimates, respectively. We compare our main specification with one in which the coefficients associated with DVP and UVP are homogeneous, which is equivalent to a regression for the predictability of the total variance premium (VP):

$$\kappa^{-1}r_{t,t+\kappa}^i = a_\kappa + b_\kappa(vp_{t,t+1}^D + vp_{t,t+1}^U) + \epsilon_{i,t+\kappa}.$$

In both specifications, the coefficients are estimated using ordinary least squares, where the coefficients associated with VP and its components are restricted to be homogeneous across countries. The VP estimated coefficients and their  $h$ -lag corrected Newey-West standard errors (SE, in parentheses) are reported along with the adjusted  $R^2$ . “VARC” indicates the variance decomposition of the model. \*\*\*, \*\*, and \* represent significance at the 1%, 5%, and 10% confidence levels.

	$\kappa=1$	$\kappa=3$	$\kappa=6$	$\kappa=12$
$vp$	0.119	0.265***	0.313***	0.160***
(SE)	(0.137)	(0.089)	(0.067)	(0.053)
$vp^D$	-0.011	0.215***	0.299***	0.179***
(SE)	(0.137)	(0.089)	(0.067)	(0.052)
[VARC%]	[0.0%]	[43.1%]	[83.8%]	[98.0%]
$vp^U$	2.100***	1.020***	0.526***	-0.116
(SE)	(0.374)	(0.297)	(0.181)	(0.183)
[VARC%]	[100%]	[56.9%]	[16.2%]	[2.0%]
Adj. $R^2$	0.04%	0.66%	1.67%	0.85%
	<b>0.82%</b>	<b>0.96%</b>	<b>1.71%</b>	<b>0.99%</b>

Table 4: Country-level economic and financial exposures

This table presents the time-series averages of our proxies for country-level exposure to global risks. We use the trade-to-GDP ratio (source: World Bank, 1990 to 2018) as the proxy for a country’s economic exposure and the average total equity and debt security holdings from/to country  $i$  to/from the rest of the world (source: IMF, The Coordinated Portfolio Investment Survey, 2001 to 2018) as the proxy for a country’s financial exposure (Schularick and Steger (2010)). We report the average ratio in percentages (“Ratio (%)”) and the average proportion with respect to the United States (“Prop. to U.S.”). We also provide a within-variable sort based on percentiles for each variable: low, [0th, 33rd); middle, [33rd,67th); high, [67th,100th].

	Trade-to-GDP			Holdings-to-GDP		
	Ratio (%)	Prop. to U.S.	L/M/H	Ratio (%)	Prop. to U.S.	L/M/H
Australia	39.83	1.60	L	106.86	1.17	L
Austria	88.24	3.51	M	171.78	1.96	H
Belgium	139.71	5.59	H	235.97	2.68	H
Canada	66.53	2.70	L	121.02	1.30	M
Denmark	86.31	3.43	M	178.42	1.90	M
Finland	69.74	2.78	M	211.84	2.35	M
France	52.74	2.11	M	189.13	2.08	L
Germany	66.41	2.61	M	148.07	1.66	M
Hong Kong	315.16	12.42	H	450.49	4.74	H
Ireland	163.12	6.48	H	1,185.89	12.71	H
Italy	48.60	1.94	L	121.86	1.39	L
Japan	25.14	0.99	L	86.32	0.92	L
Netherlands	125.27	5.00	H	396.21	4.43	H
Norway	70.08	2.85	M	63.61	0.71	M
New Zealand	58.01	2.36	L	223.50	2.31	M
Portugal	67.68	2.71	M	141.00	1.62	M
Singapore	353.76	14.28	H	329.81	3.60	H
Spain	53.40	2.13	L	114.65	1.30	L
Sweden	76.67	3.06	M	190.78	2.10	M
Switzerland	100.05	3.98	H	302.79	3.47	H
United Kingdom	53.74	2.16	H	236.11	2.60	L
United States	25.08	1.00	L	93.68	1.00	L

Table 5: Country-level exposure and predictability patterns

This table shows the results for the following regression setting:

$$\begin{aligned} \kappa^{-1} r_{t,t+\kappa}^i = & a_\kappa + (b_\kappa^D + b_{EE,\kappa}^D EE^i + b_{FE,\kappa}^D FE^i) vp_{t,t+1}^D \\ & + (b_\kappa^U + b_{EE,\kappa}^U EE^i + b_{FE,\kappa}^U FE^i) vp_{t,t+1}^U + \epsilon_{i,t+\kappa}, \end{aligned}$$

where  $EE^i$  and  $FE^i$  are the time-series averages of our proxies for economic and financial exposure, respectively, which are described in Table 4. \*\*\*, \*\*, and \* represent significance at the 1%, 5%, and 10% confidence levels. Robustness tests using time-varying exposure measures and alternative financial exposure measures are presented in Tables A3 and A4.

	$b_\kappa^D$	$b_{EE,\kappa}^D$	$b_{FE,\kappa}^D$	$b_\kappa^U$	$b_{EE,\kappa}^U$	$b_{FE,\kappa}^U$	$R^2$
$\kappa = 1$	0.005 (0.151)	0.022 (0.018)	-0.040 (0.026)	1.992*** (0.482)	-0.078 (0.080)	0.161 (0.148)	0.838
$\kappa = 2$	0.199* (0.111)	0.023* (0.013)	-0.039** (0.018)	0.955** (0.390)	-0.116** (0.056)	0.164* (0.092)	0.584
$\kappa = 3$	0.216** (0.094)	0.020* (0.011)	-0.032** (0.015)	1.156*** (0.337)	-0.082 (0.054)	0.072 (0.087)	1.028
$\kappa = 4$	0.232*** (0.082)	0.020** (0.009)	-0.033** (0.014)	1.413*** (0.334)	-0.078 (0.051)	0.046 (0.089)	1.725
$\kappa = 5$	0.273*** (0.071)	0.019*** (0.007)	-0.033*** (0.011)	1.036*** (0.240)	-0.065* (0.038)	0.043 (0.058)	1.729
$\kappa = 6$	0.309*** (0.068)	0.019*** (0.006)	-0.033*** (0.009)	0.663*** (0.201)	-0.060** (0.030)	0.038 (0.042)	1.861
$\kappa = 7$	0.300*** (0.066)	0.019*** (0.006)	-0.034*** (0.008)	0.368* (0.190)	-0.055* (0.031)	0.048 (0.042)	1.792
$\kappa = 8$	0.250*** (0.068)	0.019*** (0.006)	-0.034*** (0.008)	0.312* (0.189)	-0.052 (0.032)	0.051 (0.039)	1.447
$\kappa = 9$	0.231*** (0.064)	0.018*** (0.006)	-0.034*** (0.007)	0.036 (0.198)	-0.037 (0.034)	0.038 (0.038)	1.289
$\kappa = 10$	0.206*** (0.061)	0.018*** (0.005)	-0.033*** (0.007)	-0.026 (0.204)	-0.033 (0.030)	0.033 (0.034)	1.173
$\kappa = 11$	0.200*** (0.056)	0.018*** (0.004)	-0.033*** (0.006)	-0.084 (0.201)	-0.029 (0.027)	0.028 (0.030)	1.251
$\kappa = 12$	0.192*** (0.051)	0.018*** (0.004)	-0.033*** (0.006)	-0.076 (0.183)	-0.034 (0.024)	0.037 (0.028)	1.297

Table 6: Summary statistics for international variance premium components

This table reports time series averages, standard deviations (SDs), and minimum and maximum values of the monthly downside (panel A) and upside (panel B) variance premiums (DVP and UVP, respectively) for the United States, Germany, France, and Switzerland, as well as the equal-weighted average across all countries, which we label as “Global avg.” All measures are in units of monthly variance—i.e., in annual percentage squared divided by 12 (as commonly used in the literature; see, e.g., Bekaert and Hoerova (2014) and Kilic and Shaliastovich (2019)). We also report correlations across countries for downside (panel C) and upside (panel D) variance premiums. The sample runs from April 2003 to December 2019.

	U.S.	Germany	France	Switzerland	Global avg.
Panel A. DVP summary statistics					
$Mean(vp_{t,t+1}^D)$	16.110	12.440	19.675	12.186	15.103
$SD(vp_{t,t+1}^D)$	1.016	0.821	1.199	0.868	0.906
$Min(vp_{t,t+1}^D)$	3.514	-13.402	-8.966	-4.654	-5.349
$Max(vp_{t,t+1}^D)$	93.054	90.335	118.407	119.244	105.260
Panel B. UVP summary statistics					
$Mean(vp_{t,t+1}^U)$	0.794	0.097	1.041	0.412	0.586
$SD(vp_{t,t+1}^U)$	0.256	0.185	0.328	0.244	0.226
$Min(vp_{t,t+1}^U)$	-35.484	-25.172	-37.739	-34.511	-33.227
$Max(vp_{t,t+1}^U)$	8.660	4.572	20.559	7.627	7.673
Panel C. DVP correlations					
U.S.	1				
Germany	0.850	1			
France	0.896	0.930	1		
Switzerland	0.851	0.905	0.899	1	
Global avg.	0.944	0.957	0.976	0.950	1
Panel D. UVP correlations					
U.S.	1				
Germany	0.871	1			
France	0.759	0.805	1		
Switzerland	0.720	0.748	0.759	1	
Global avg.	0.909	0.923	0.929	0.883	1



Table 7: The international predictability of U.S. and global average VP and its components

This table reports evidence for the ability of the variance premium (VP) and its components to predict international stock returns at various horizons of interest (in units of months). Our specification is the following:

$$\kappa^{-1}r_{t,t+\kappa}^i = a_\kappa + b_\kappa^D vp_{t,t+1}^D + b_\kappa^U vp_{t,t+1}^U + \epsilon_{i,t+\kappa},$$

where  $r_{t,t+\kappa}^i$  denotes the  $\kappa$ -month-ahead log excess returns for country  $i$  and  $vp_{t,t+1}^D$  and  $vp_{t,t+1}^U$  denote downside and upside (DVP and UVP) estimates, respectively. We compare the predictive power of the U.S. VP components with that of the global average of the VP components calculated as the equally-weighted average of the VP components of the United States, Germany, France, and Switzerland. The coefficients are estimated using ordinary least squares, where the coefficients associated with VP and its components are restricted to be homogeneous across countries. The VP estimated coefficients and their  $h$ -lag corrected Newey-West standard errors (in parentheses) are reported along with the adjusted  $R^2$ . “VARC” indicates the variance decomposition of the model. \*\*\*, \*\*, and \* represent significance at the 1%, 5%, and 10% confidence levels. The sample runs from April 2003 to December 2019.

	$\kappa=1$		$\kappa=3$		$\kappa=6$		$\kappa=12$	
	U.S.	Global avg.	U.S.	Global avg.	U.S.	Global avg.	U.S.	Global avg.
$vp^D$	0.120	0.204	0.222*	0.268*	0.380***	0.560***	0.214***	0.380***
(SE)	(0.186)	(0.206)	(0.120)	(0.145)	(0.085)	(0.087)	(0.065)	(0.060)
[VARC%]	[0.3%]	[-0.9%]	[24.9%]	[11.2%]	[78.5%]	[57.1%]	[92.1%]	[85.8%]
$vp^U$	3.233***	3.465***	1.478***	2.193***	0.909***	2.048***	-0.210	0.829**
(SE)	(0.502)	(0.529)	(0.398)	(0.438)	(0.238)	(0.308)	(0.218)	(0.329)
[VARC%]	[99.7%]	[100.9%]	[75.1%]	[88.8%]	[21.5%]	[42.9%]	[7.9%]	[14.2%]
Adj. $R^2$	2.41%	2.20%	1.56%	2.32%	2.87%	5.64%	1.84%	4.11%

Table 8: Summary statistics for risk premium state variables

This table provides summary statistics for the three risk premium state variables introduced in Section 3.2: good and bad economic uncertainty ( $\theta p_t$  and  $\theta n_t$ , respectively) and expected risk aversion fluctuations ( $qh_t$ ). The full sample estimation results and detailed dynamic processes are available in Appendix C. \*\*\*, \*\*, and \* represent significance at the 1%, 5%, and 10% confidence levels. The summary statistics are calculated for a sample running from April 1991 to December 2019.

	$\theta p_t$	$\theta n_t$	$qh_t$
Panel A. Univariate statistics			
Mean	476.020	3.342	0.838
SD	15.176	7.798	1.107
Skewness	0.724	5.133	3.379
AR(1)	0.972	0.911	0.500
Panel B. Correlation matrix			
$\theta p_t$	1		
$\theta n_t$	-0.222***	1	
$qh_t$	-0.070	0.191***	1
NBER	-0.182***	0.532***	0.205***
Cyclicalilty	Pro-	Counter-	Counter-

Table 9: Model fit: VP component dynamics

This table presents the moment matching results of the GMM system used to estimate the loadings of downside and upside variance premiums (DVP and UVP, respectively) on the five risk premium state variables (see details in Section 3.1). This GMM system has 14 unknowns and 50 moments and is estimated using iterative GMM. \*\*\*, \*, and \* indicate that the model estimate is, respectively, within 1.645, 1.96, and 2.576 standard deviations (SDs) of the empirical point estimate in the same row. Standard model specification statistics and empirical correlations are shown at the end of the table, and the correlations are both statistically different from zero at a 95% test.

	Moment	Empirical	Boot. SE	Model
1	$vp^D$	15.972	(0.725)	16.795***
2	$vp^U$	1.265	(0.173)	1.39***
3	$(vp^D - E(vp^D))^2$	182.198	(33.504)	183.457***
4	$(vp^U - E(vp^U))^2$	10.755	(4.230)	10.744***
5	$(vp^D - E(vp^D))^3 / (SD(vp^D)^3)$	2.656	(0.885)	2.825***
6	$(vp^U - E(vp^U))^3 / (SD(vp^U)^3)$	-5.001	(3.959)	-4.438***
7	$(vp^D - E(vp^D))^4 / (SD(vp^D)^4)$	12.293	(4.287)	12.047***
8	$(vp^U - E(vp^U))^4 / (SD(vp^U)^4)$	53.202	(45.926)	52.268***
9	$(vp^D - E(vp^D)) * (vp^U - E(vp^U))$	1.262	(8.555)	1.17***
10	$vp^D / (vp^D + vp^U)$	0.927	(0.010)	0.918***
GMM J Statistics:				36.93
DF:				36
Hansen's overidentification test, p-value:				0.43
Dynamic correlation with empirical estimates, DVP:				0.8518
Dynamic correlation with empirical estimates, UVP:				0.4675

Table 10: Model fit: VP component predictive coefficients

This table provides the model fit results of the international stock return predictive coefficients of the variance premium (VP) components (see details in Section 3.1). Panels A and B report the average, median, and cross-country variations of the downside and upside variance premiums' (DVP and UVP, respectively) predictive coefficients, respectively, and provide closeness tests with their empirical counterparts; \*\*\*, \*\*, and \* indicate that the model estimate is, respectively, within the 1.645, 1.96, and 2.576 standard deviations (SDs) of the empirical point estimate in the same row.

Panel A.	Average DVP coeff.			Median DVP coeff.			Cross-country SD DVP coeff.		
Horizon	Emp.	SE	Mod.	Emp.	SE	Mod.	Emp.	SE	Mod.
1	-0.011	(0.052)	-0.029***	-0.036	(0.070)	-0.007***	0.245	(0.026)	0.142
2	0.188	(0.043)	0.168***	0.151	(0.048)	0.189***	0.202	(0.024)	0.137
3	0.215	(0.036)	0.200***	0.188	(0.031)	0.214***	0.171	(0.023)	0.122*
4	0.226	(0.036)	0.211***	0.221	(0.024)	0.232***	0.169	(0.026)	0.13***
5	0.262	(0.036)	0.245***	0.262	(0.030)	0.270***	0.169	(0.025)	0.128***
6	0.299	(0.036)	0.284***	0.289	(0.032)	0.308***	0.168	(0.026)	0.126***
7	0.287	(0.035)	0.275***	0.265	(0.030)	0.298***	0.166	(0.026)	0.128***
8	0.235	(0.034)	0.228***	0.220	(0.027)	0.252***	0.161	(0.027)	0.125***
9	0.214	(0.033)	0.209***	0.214	(0.023)	0.233***	0.157	(0.028)	0.122***
10	0.189	(0.033)	0.186***	0.191	(0.022)	0.210***	0.155	(0.027)	0.121***
11	0.185	(0.033)	0.182***	0.184	(0.022)	0.204***	0.153	(0.027)	0.121***
12	0.179	(0.032)	0.176***	0.174	(0.023)	0.196***	0.149	(0.025)	0.118***
Panel B.	Average UVP coeff.			Median UVP coeff.			Cross-country SD UVP coeff.		
Horizon	Emp.	SE	Mod.	Emp.	SE	Mod.	Emp.	SE	Mod.
1	2.100	(0.241)	1.955***	1.999	(0.184)	1.894***	1.128	(0.204)	0.618*
2	0.922	(0.174)	0.846***	0.995	(0.129)	0.871***	0.814	(0.143)	0.650***
3	1.020	(0.117)	0.979***	1.272	(0.144)	1.024**	0.548	(0.099)	0.419***
4	1.227	(0.106)	1.191***	1.309	(0.122)	1.244***	0.497	(0.077)	0.405***
5	0.891	(0.081)	0.873***	0.906	(0.121)	0.918***	0.380	(0.050)	0.354***
6	0.526	(0.063)	0.531***	0.551	(0.072)	0.575***	0.293	(0.045)	0.254***
7	0.276	(0.053)	0.287***	0.299	(0.081)	0.323***	0.247	(0.032)	0.225***
8	0.237	(0.053)	0.236***	0.296	(0.086)	0.267***	0.250	(0.030)	0.208***
9	-0.009	(0.045)	-0.007***	-0.009	(0.048)	0.016***	0.209	(0.031)	0.137*
10	-0.069	(0.047)	-0.066***	-0.049	(0.052)	-0.046***	0.219	(0.034)	0.118
11	-0.125	(0.048)	-0.121***	-0.122	(0.061)	-0.102***	0.225	(0.034)	0.098
12	-0.116	(0.047)	-0.119***	-0.107	(0.053)	-0.1***	0.220	(0.039)	0.117

Table 11: The dynamics of VP components and risk premium state variables

This table presents the GMM (Stage 1) estimation results and highlights the relative importance of the risk premium state variables that drive the dynamics of VP components. For each GMM iteration, the model-implied DVP and UVP ( $\widehat{vp}_t^D$  and  $\widehat{vp}_t^U$ , respectively) can be expressed as:

$$\begin{aligned}\widehat{vp}_t^D &= vp_0^D + w_{\theta p,t}^D \widehat{\theta p}_t + w_{\theta n,t}^D \widehat{\theta n}_t + w_{qh,t}^D \widehat{qh}_t, \\ \widehat{vp}_t^U &= vp_0^U + w_{\theta p,t}^U \widehat{\theta p}_t + w_{\theta n,t}^U \widehat{\theta n}_t + w_{qh,t}^U \widehat{qh}_t,\end{aligned}$$

where, for  $x \in \{\theta p, \theta n, qh\}$ ,  $\widehat{x}$  indicates the estimated risk premium state variables (Section 3.2), and  $w_{x,t}^D$  and  $w_{x,t}^U$  indicate the corresponding time-varying coefficients:

$$\begin{aligned}w_{x,t}^D &= w_{x,0}^D + w_{x,1}^D z_t, \\ w_{x,t}^U &= w_{x,0}^U + w_{x,1}^U z_t,\end{aligned}$$

where  $z_t$  is the percent-squared innovation to real monthly economic growth (unit: monthly growth innovation-squared multiplied by 10000). Standard errors are shown in parentheses and variance decomposition results are shown in the third row ("VARC"). The variance contribution is calculated as  $\frac{\beta_v \text{cov}(v_t, \widehat{y}_t)}{\widehat{y}_t} \times 100\%$ , where  $v_t$  denotes an explanatory variable,  $\beta_v$  the corresponding loading, and  $\widehat{y}_t$  the total explained  $y$  variable. \*\*\*, \*\*, and \* represent significance at the 1%, 5%, and 10% confidence levels. Constants are not reported in this table but are included in the estimation ( $vp_0^D = -49.391^{**}$  and  $vp_0^U = -25.799^{***}$ ).

	$\theta p_t$	$\theta n_t$	$qh_t$
DVP: $w_0^D$	0.113***	1.088***	9.400***
(SE)	(0.043)	(0.073)	(0.333)
[VARC%]	-0.23%	38.98%	63.71%
$w_1^D$	0.012***	-0.162***	-0.153
	(0.001)	(0.006)	(0.106)
	18.70%	-19.01%	-2.15%
UVP: $w_0^U$	0.058***	0.278***	0.438***
	(0.009)	(0.013)	(0.102)
	4.12%	0.55%	-0.75%
$w_1^U$	-0.009***	0.001	0.203***
	(2.5E-04)	(0.003)	(0.043)
	117.52%	-0.78%	-20.68%

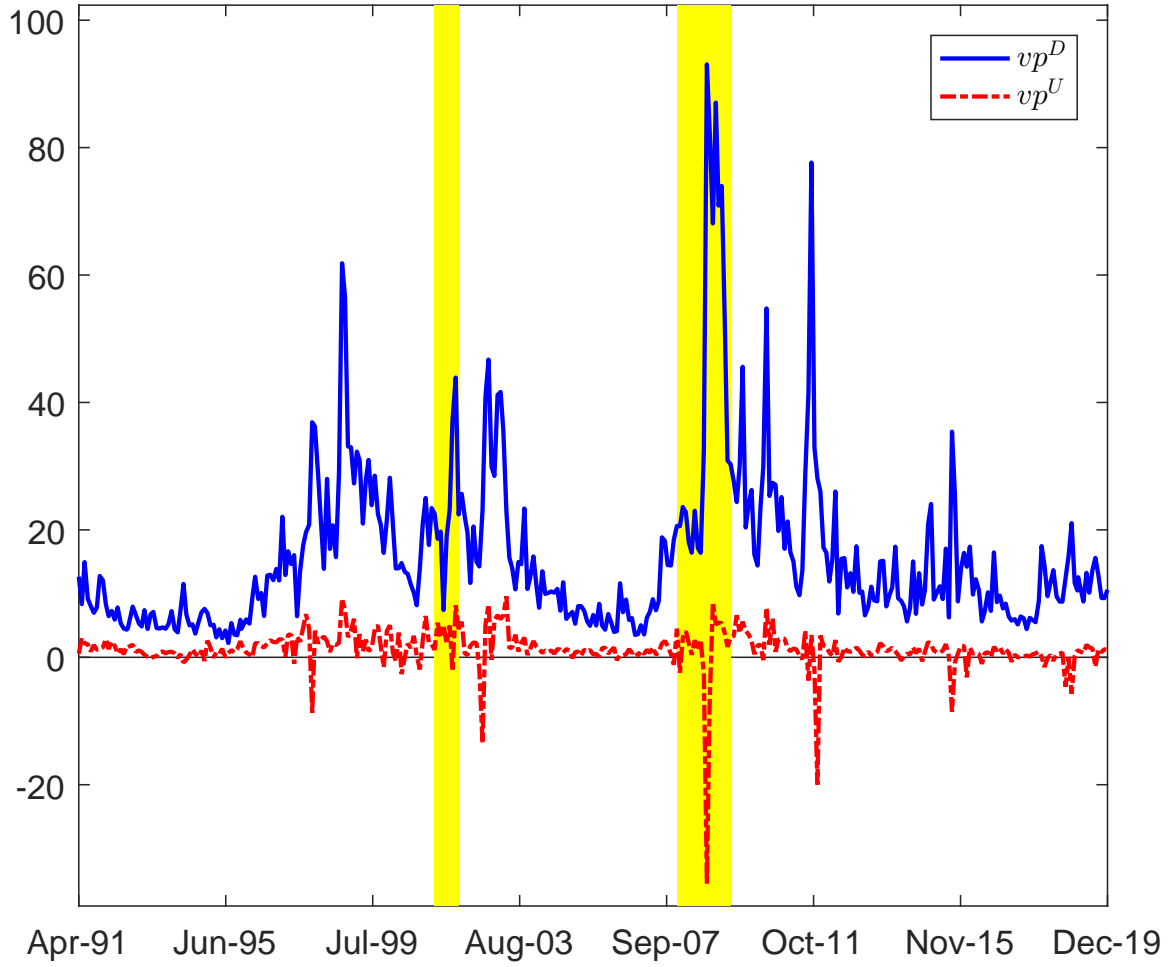


Figure 1: Downside and upside components of the variance risk premium

This figure shows the time series of the downside and upside variance premium components. The construction details of variance risk premiums are discussed in Section 2. The downside (upside) variance risk premium is calculated as the difference between the option-implied downside (upside) variance and the expected downside (upside) realized variance. We use the best forecasts of the downside and upside realized variances from Table 1 (specification (5)). Measures are in units of monthly percentages.

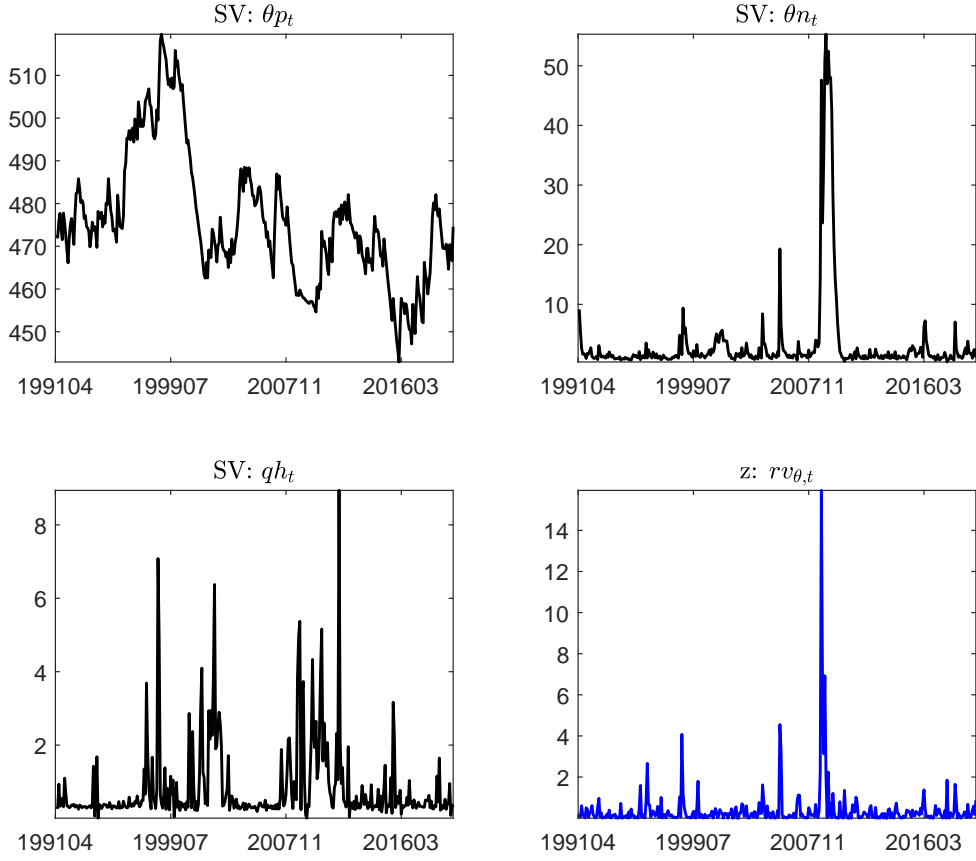


Figure 2: State variable dynamics

This figure shows the dynamics of the estimated risk premium state variables (good and bad economic uncertainty,  $\theta_{p_t}$  and  $\theta_{n_t}$ , and expected risk aversion fluctuations,  $qh_t$ ) and the time-varying loading instrument (monthly realized variance of economic growth,  $z_t$ , multiplied by 10000) from April 1991 to December 2019. The corresponding summary statistics are shown in Table 8. The full sample estimation results and detailed dynamic processes are available in Internet Appendix C.

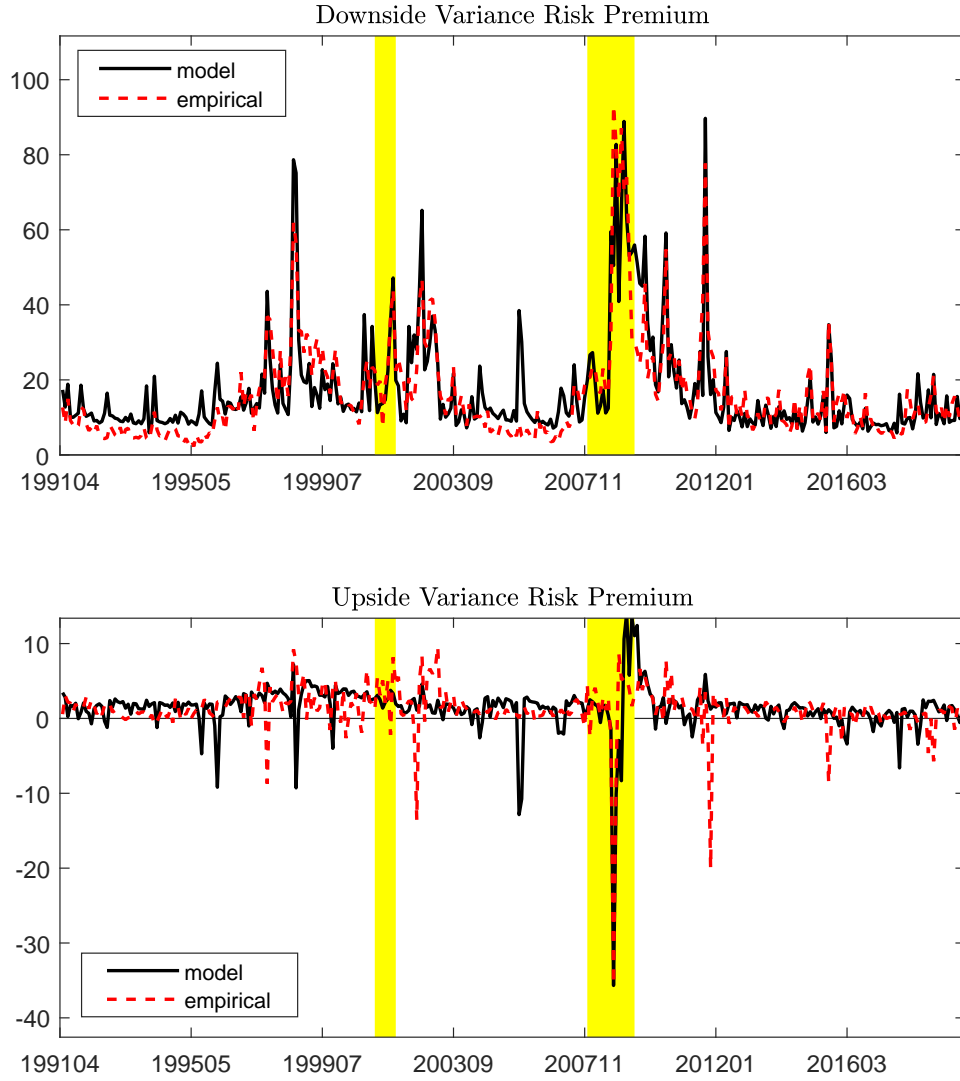
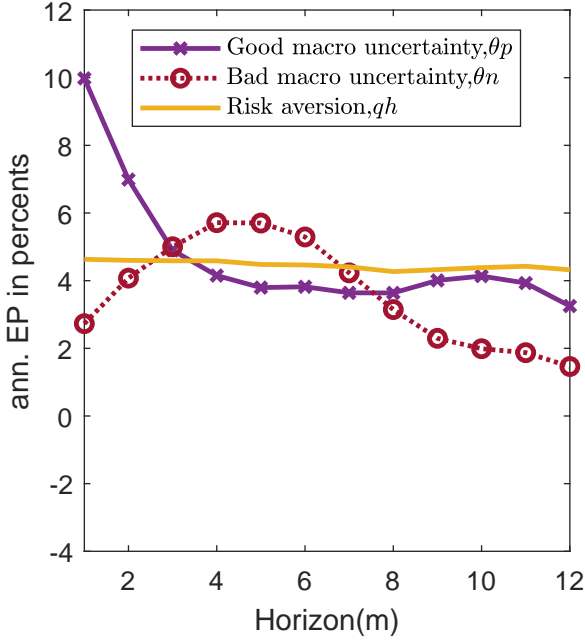


Figure 3: Dynamic fit

This figure shows the dynamics of empirical and model-implied downside variance premium (DVP, top panel) and upside variance premium (UVP, bottom panel) estimates. The dashed red lines depict the empirical estimates as obtained from Section 2. The solid black lines depict the model-implied estimates; the correlations with the DVP and UVP empirical estimates are 0.85 and 0.47, respectively. Other estimation details are shown in Table 9.

(A). Changes in EP given 1SD increase in S.V.



(B). EP variance decompositon

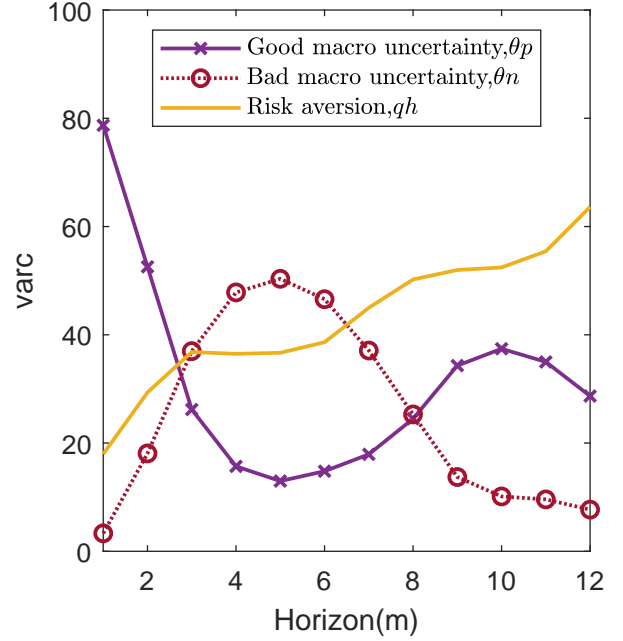


Figure 4: Economic effects of risk premium state variables (S.V.s) on international equity risk premiums: An average-country view

Panel (A) shows the model-implied effect of a one standard deviation (SD) increase in a U.S./global risk premium state variable on an average country's equity risk premium (EP), where an average country is calibrated with *median* economic exposure  $EE^i$  (the ratio of country  $i$ 's and the U.S.'s international trade-to-GDP) and *median* financial exposure  $FE^i$  (the ratio of country  $i$ 's and the U.S.'s international holding-to-GDP); see construction and data details in Table 4. EP is expressed in annualized percentages for all horizons. The average value of  $z_t$  is used. Panel (B) shows the variance decomposition (in percentages) of the model-implied international EPs at various horizons coming from different sources of state variables; by construction, at each horizon, the sum of the three numbers sum to 100%.



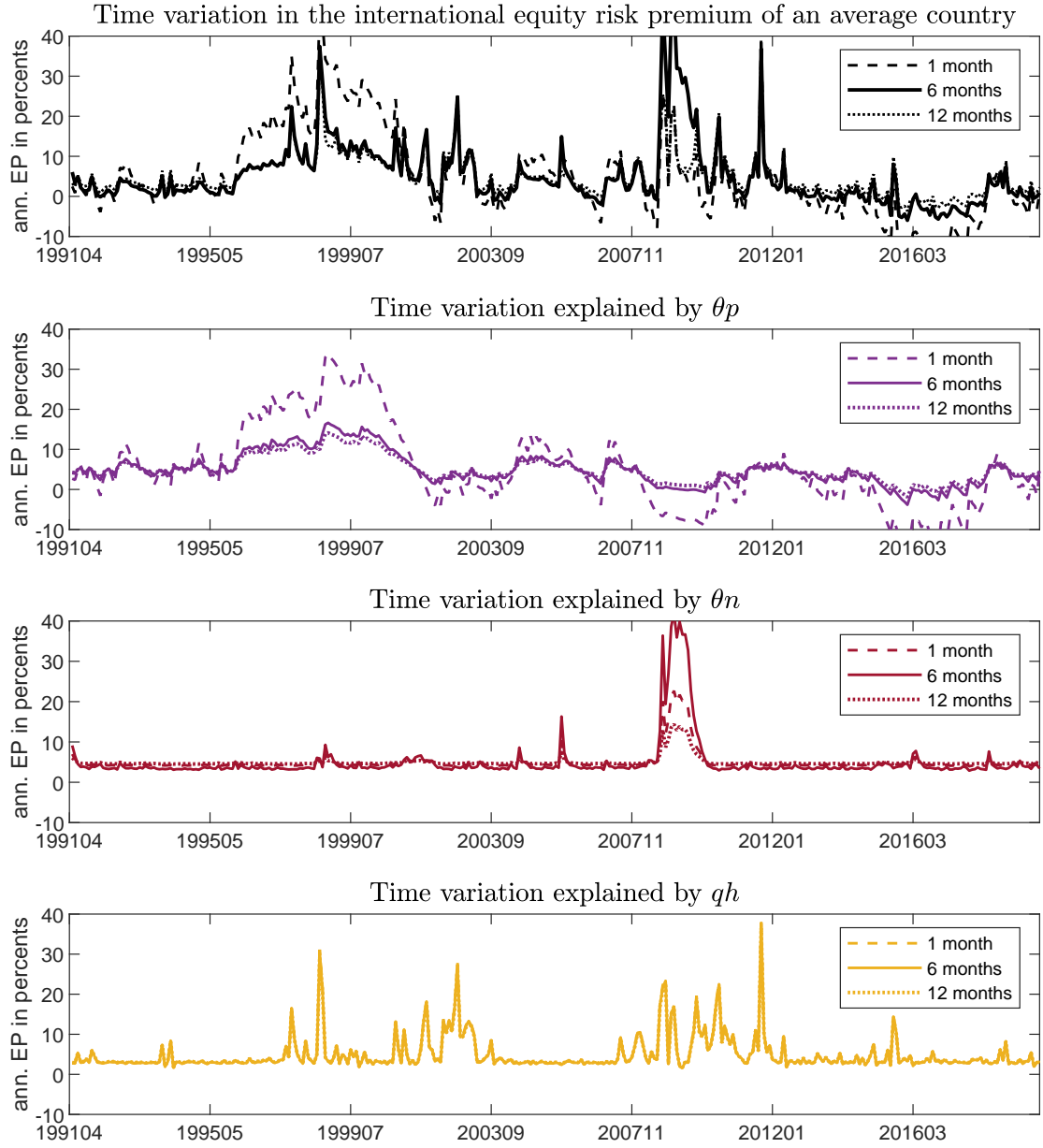


Figure 5: Time variation in the model-implied international equity risk premium

The first plot shows the time variation in the model-implied international equity risk premium for an average country (with median economic and financial exposure). The international equity risk premium means the compensation demanded due to global risks, and it is expressed in annualized percentages in this plot. The next three plots present a dynamic breakdown, showing how the time variation of the international equity risk premium would behave if we keep the dynamics of one state variable and mute the dynamics from the other two state variables, without re-estimation: from top to bottom, good macro uncertainty  $\theta p_t$ , bad macro uncertainty  $\theta n_t$ , and risk aversion  $qh_t$ . Finally, in each plot, we show international equity risk premiums over several representative horizons of interest: 1 month (dashed), 6 months (solid), 12 months (dotted).

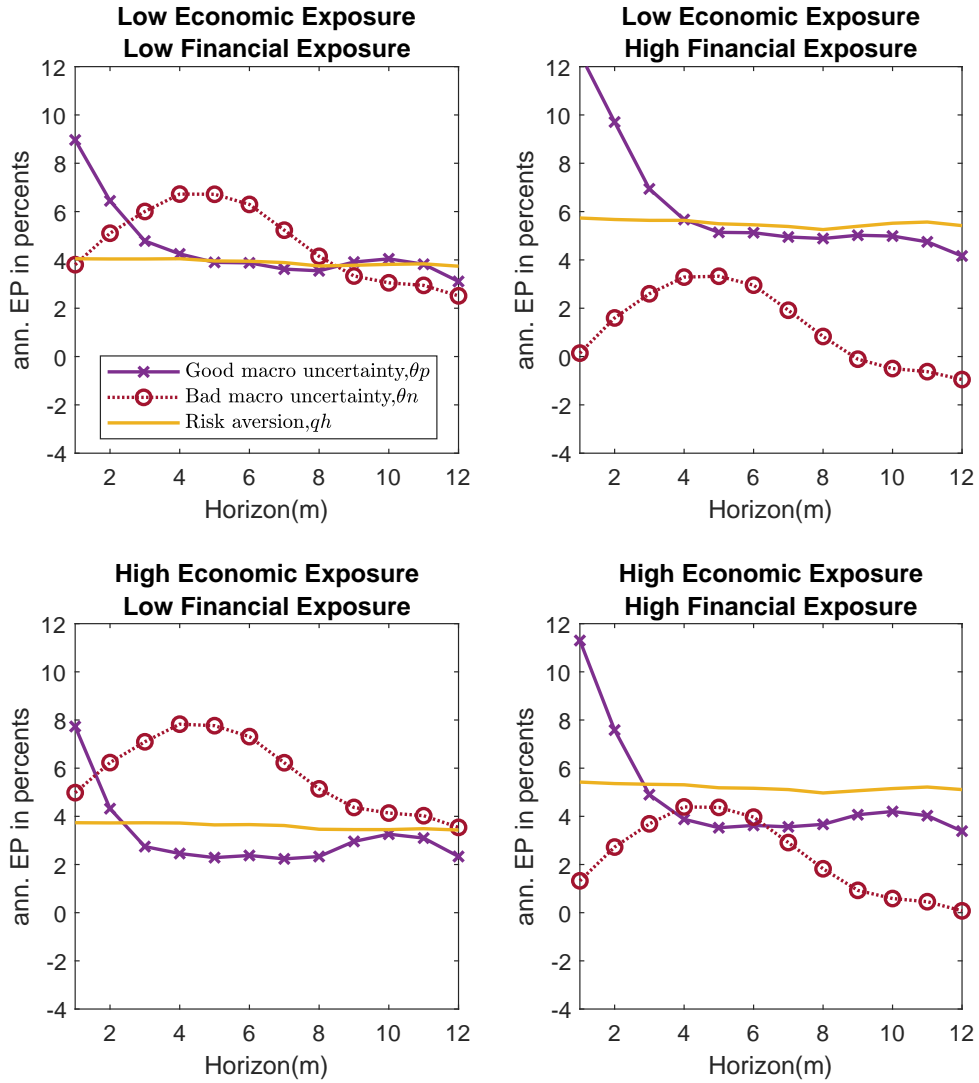


Figure 6: Economic effects of risk premium state variables on international equity risk premiums: A cross-country view

This figure complements Figure 4-(A) with a cross-country view, showing the effect of a one standard deviation (SD) increase in a common premium state variable on international equity risk premiums. The results are calibrated using low and high economic and financial exposure, with low (high) being those countries with exposure below the 33rd (above the 67th) percentile value of the 22 countries; see construction and data details in Table 4. The EP is expressed in annualized percentages for all horizons. A cross-country version of Figure 4-(B) is shown in Appendix C of the Internet Appendix.

# INTERNET APPENDICES

## A. Additional tables and figures for Section 2

Table A1: Expected realized variance

This table shows the coefficients associated with the predictors of one-month-ahead (22 days) total realized variance. The specifications are similar to those for realized semivariances in Table 1. The specification in column (1) assumes that the realized variance follow a Martingale ( $E_t(rv_{t+1m}) = rv_t$ ). For the specifications in columns (2) to (5), we estimate the following regression setting:  $E_t(rv_{t+1}) = \hat{\alpha} + \hat{\gamma}\mathbf{G}_t$ . We consider the following predictors in matrix  $\mathbf{G}$ : the total realized variance calculated over the last month ( $rv_{t-1m,t}$ ); realized variance calculated using either the last five days ( $rv_{t-5d,t}$ ) or the last day of the month ( $rv_{t-1d,t}$ ); and the option-implied variance ( $iv_{t,t+1m}$ ). We report, in parentheses, heteroskedasticity and autocorrelation consistent (HAC) standard deviations with 44 lags. \*\*\*, \*\*, and \* represent significance at the 1%, 5%, and 10% confidence levels. The adjusted  $R^2$ s are reported at the end of the table.

	(1)	(2)	(3)	(4)	(5)
Constant	0	7.72***	7.72***	6.96***	4.15***
	-	(1.28)	(1.28)	(1.10)	(1.56)
$rv_{t-1m,t}$	1	0.64***	0.64***	0.27***	0.12
	-	(0.08)	(0.08)	(0.10)	(0.09)
$rv_{t-5d,t}$				0.32**	0.29*
				(0.16)	(0.17)
$rv_{t-1d,t}$				0.09***	0.06**
				(0.02)	(0.02)
$iv_{t,t+1m}$					0.21*
					(0.12)
Adj. $R^2$	0.270	0.406	0.406	0.466	0.474

Table A2: Correlations

This table reports correlations among the monthly U.S. downside and upside variance premiums (DVP and UVP, respectively) across various measures. Models are reported in Table 1. Panel A (Panel B) reports correlations of DVP (UVP) estimates across measures. The sample runs from April 1991 to December 2019.

(1)	(2)	(3)	(4)	(5)	
A. Correlations across models; DVP					
(1)	1				
(2)	0.87	1			
(3)	0.87	0.99	1		
(4)	0.77	0.97	0.97	1	
(5)	0.74	0.97	0.96	0.99	1

(1)	(2)	(3)	(4)	(5)	
B. Correlations across models; UVP					
(1)	1				
(2)	0.80	1			
(3)	0.77	0.94	1.00		
(4)	0.77	0.90	0.88	1	
(5)	0.77	0.74	0.75	0.95	1

Table A3: Country-level exposure and predictability patterns, time-varying exposure

This table shows the results for the following regression setting:

$$\kappa^{-1}r_{t,t+\kappa}^i = a_\kappa + (b_\kappa^D + b_{EE,\kappa}^D EE_{t-1}^i + b_{FE,\kappa}^D FE_{t-1}^i)vp_{t,t+1}^D + (b_\kappa^U + b_{EE,\kappa}^U EE_{t-1}^i + b_{FE,\kappa}^U FE_{t-1}^i)vp_{t,t+1}^U + \epsilon_{i,t+\kappa},$$

where  $EE^i$  and  $FE^i$  are our proxies for economic and financial exposure, respectively; they are described in Table 4. These variables are available at an annual frequency, and they are converted to monthly frequency using a step function. \*\*\*, \*\*, and \* represent significance at the 1%, 5%, and 10% confidence levels.

	$b_\kappa^D$	$b_{EE,\kappa}^D$	$b_{FE,\kappa}^D$	$b_\kappa^U$	$b_{EE,\kappa}^U$	$b_{FE,\kappa}^U$	$R^2$
$\kappa = 1$	0.004 (0.153)	0.023 (0.018)	-0.039 (0.026)	2.050*** (0.488)	-0.092 (0.080)	0.158 (0.158)	0.836
$\kappa = 2$	0.197* (0.112)	0.021* (0.012)	-0.035* (0.018)	0.876** (0.383)	-0.115** (0.057)	0.188* (0.099)	0.570
$\kappa = 3$	0.205** (0.096)	0.019* (0.010)	-0.023 (0.015)	1.101*** (0.340)	-0.085 (0.054)	0.097 (0.091)	0.995
$\kappa = 4$	0.218*** (0.083)	0.019** (0.009)	-0.024* (0.013)	1.363*** (0.338)	-0.088* (0.050)	0.080 (0.089)	1.677
$\kappa = 5$	0.260*** (0.073)	0.017** (0.007)	-0.023** (0.010)	0.977*** (0.242)	-0.067* (0.038)	0.069 (0.060)	1.659
$\kappa = 6$	0.297*** (0.070)	0.017*** (0.006)	-0.024*** (0.009)	0.599*** (0.204)	-0.065** (0.031)	0.071* (0.043)	1.789
$\kappa = 7$	0.288*** (0.068)	0.017*** (0.006)	-0.025*** (0.008)	0.285 (0.189)	-0.060* (0.032)	0.087* (0.045)	1.709
$\kappa = 8$	0.237*** (0.070)	0.017*** (0.006)	-0.025*** (0.007)	0.220 (0.186)	-0.058* (0.033)	0.095** (0.041)	1.361
$\kappa = 9$	0.217*** (0.066)	0.016*** (0.006)	-0.025*** (0.007)	-0.049 (0.191)	-0.044 (0.035)	0.083** (0.041)	1.189
$\kappa = 10$	0.193*** (0.063)	0.017*** (0.005)	-0.026*** (0.006)	-0.125 (0.194)	-0.042 (0.031)	0.086** (0.038)	1.079
$\kappa = 11$	0.188*** (0.057)	0.017*** (0.004)	-0.026*** (0.006)	-0.184 (0.190)	-0.040 (0.027)	0.084** (0.035)	1.158
$\kappa = 12$	0.181*** (0.052)	0.017*** (0.004)	-0.026*** (0.005)	-0.179 (0.172)	-0.045* (0.024)	0.093*** (0.032)	1.214

Table A4: Country-level exposure and predictability patterns, alternative financial exposure proxies

This table shows the results for the following regression setting:

$$\begin{aligned} \kappa^{-1}r_{t,t+\kappa}^i = & a_\kappa + (b_\kappa^D + b_{EE,\kappa}^D EE^i + b_{FE,\kappa}^D FE^i)vp_{t,t+1}^D \\ & + (b_\kappa^U + b_{EE,\kappa}^U EE^i + b_{FE,\kappa}^U FE^i)vp_{t,t+1}^U + \epsilon_{i,t+\kappa}, \end{aligned}$$

where  $EE^i$  and  $FE^i$  are the time-series averages of our proxies for economic and financial exposure, respectively. We consider three alternative proxies for financial exposure: the ratio of international bank claims to GDP (source: BIS, in panel A), the capital market restriction index in Fernandez et al. (2016) (panel B), and the equity market domestic investment share (source: IMF, coordinated portfolio investment survey, in panel C). \*\*\*, \*\*, and \* represent significance at the 1%, 5%, and 10% confidence levels.

Panel A. International bank claims

	$b_\kappa^D$	$b_{EE,\kappa}^D$	$b_{FE,\kappa}^D$	$b_\kappa^U$	$b_{EE,\kappa}^U$	$b_{FE,\kappa}^U$	$R^2$
$\kappa = 1$	-0.039 (0.150)	0.009 (0.047)	-0.001 (0.025)	2.143*** (0.446)	0.208 (0.207)	-0.135 (0.113)	0.834
$\kappa = 2$	0.148 (0.110)	0.022 (0.033)	-0.008 (0.017)	1.170*** (0.372)	0.041 (0.157)	-0.060 (0.084)	0.524
$\kappa = 3$	0.170* (0.093)	0.027 (0.027)	-0.010 (0.015)	1.272*** (0.342)	-0.037 (0.143)	-0.012 (0.078)	0.975
$\kappa = 4$	0.180** (0.080)	0.027 (0.023)	-0.010 (0.013)	1.501*** (0.342)	-0.056 (0.137)	-0.005 (0.076)	1.637
$\kappa = 5$	0.220*** (0.070)	0.027 (0.019)	-0.011 (0.011)	1.135*** (0.250)	-0.060 (0.101)	0.004 (0.056)	1.616
$\kappa = 6$	0.255*** (0.067)	0.029* (0.016)	-0.012 (0.009)	0.771*** (0.205)	-0.089 (0.070)	0.023 (0.039)	1.707
$\kappa = 7$	0.245*** (0.065)	0.028** (0.014)	-0.012 (0.008)	0.482** (0.196)	-0.091 (0.061)	0.030 (0.032)	1.583
$\kappa = 8$	0.196*** (0.066)	0.025* (0.014)	-0.010 (0.007)	0.424** (0.199)	-0.072 (0.057)	0.020 (0.029)	1.208
$\kappa = 9$	0.179*** (0.063)	0.023* (0.013)	-0.010 (0.007)	0.134 (0.210)	-0.068 (0.058)	0.025 (0.029)	1.019
$\kappa = 10$	0.156*** (0.060)	0.021* (0.012)	-0.009 (0.006)	0.063 (0.208)	-0.060 (0.056)	0.021 (0.029)	0.873
$\kappa = 11$	0.149*** (0.055)	0.021* (0.011)	-0.008 (0.006)	0.003 (0.203)	-0.063 (0.054)	0.024 (0.028)	0.920
$\kappa = 12$	0.144*** (0.051)	0.020** (0.010)	-0.008 (0.006)	0.015 (0.187)	-0.055 (0.049)	0.018 (0.026)	0.949

Table A4: Country-level exposure and predictability patterns, alternative financial exposure proxies, continued

Panel B. Capital restrictions

	$b_{\kappa}^D$	$b_{EE,\kappa}^D$	$b_{FE,\kappa}^D$	$b_{\kappa}^U$	$b_{EE,\kappa}^U$	$b_{FE,\kappa}^U$	$R^2$
$\kappa = 1$	-0.068 (0.163)	0.008 (0.016)	0.033 (0.104)	1.846*** (0.536)	-0.015 (0.068)	0.436 (0.427)	0.794
$\kappa = 2$	0.114 (0.119)	0.010 (0.011)	0.051 (0.069)	1.051** (0.432)	-0.056 (0.054)	0.125 (0.314)	0.488
$\kappa = 3$	0.152 (0.098)	0.010 (0.009)	0.035 (0.054)	1.009*** (0.366)	-0.052 (0.043)	0.301 (0.274)	0.967
$\kappa = 4$	0.156* (0.084)	0.009 (0.007)	0.047 (0.046)	1.303*** (0.368)	-0.058 (0.036)	0.214 (0.263)	1.637
$\kappa = 5$	0.188** (0.073)	0.008 (0.005)	0.061 (0.038)	1.069*** (0.271)	-0.050* (0.028)	0.023 (0.175)	1.617
$\kappa = 6$	0.225*** (0.069)	0.008 (0.005)	0.059* (0.033)	0.696*** (0.224)	-0.046** (0.023)	0.015 (0.133)	1.727
$\kappa = 7$	0.218*** (0.067)	0.008 (0.005)	0.055* (0.031)	0.395* (0.209)	-0.037 (0.023)	0.038 (0.119)	1.616
$\kappa = 8$	0.168** (0.069)	0.007 (0.005)	0.054* (0.030)	0.381* (0.212)	-0.034 (0.025)	-0.012 (0.116)	1.242
$\kappa = 9$	0.151** (0.066)	0.007 (0.005)	0.052* (0.027)	0.073 (0.225)	-0.023 (0.026)	0.011 (0.117)	1.065
$\kappa = 10$	0.125* (0.064)	0.006 (0.004)	0.054** (0.026)	0.008 (0.234)	-0.021 (0.024)	0.006 (0.120)	0.933
$\kappa = 11$	0.119** (0.059)	0.007* (0.004)	0.055** (0.023)	-0.036 (0.232)	-0.019 (0.021)	-0.021 (0.115)	0.994
$\kappa = 12$	0.114** (0.054)	0.007** (0.003)	0.053*** (0.020)	-0.031 (0.212)	-0.021 (0.018)	-0.003 (0.099)	1.023

Table A4: Country-level exposure and predictability patterns, alternative financial exposure proxies, continued

Panel C. Domestic investment share							
	$b_{\kappa}^D$	$b_{EE,\kappa}^D$	$b_{FE,\kappa}^D$	$b_{\kappa}^U$	$b_{EE,\kappa}^U$	$b_{FE,\kappa}^U$	$R^2$
$\kappa = 1$	-0.029 (0.263)	0.008 (0.016)	-0.019 (0.257)	2.913** (1.225)	-0.013 (0.067)	-1.000 (1.439)	0.788
$\kappa = 2$	0.210 (0.183)	0.009 (0.011)	-0.078 (0.174)	1.397 (0.924)	-0.055 (0.052)	-0.340 (1.036)	0.481
$\kappa = 3$	0.238* (0.143)	0.010 (0.009)	-0.081 (0.134)	1.378** (0.658)	-0.055 (0.044)	-0.188 (0.777)	0.947
$\kappa = 4$	0.257** (0.125)	0.009 (0.007)	-0.087 (0.115)	1.714*** (0.619)	-0.059 (0.036)	-0.336 (0.734)	1.620
$\kappa = 5$	0.305*** (0.107)	0.008 (0.006)	-0.096 (0.093)	1.212*** (0.429)	-0.049* (0.028)	-0.170 (0.504)	1.599
$\kappa = 6$	0.348*** (0.101)	0.008 (0.005)	-0.106 (0.079)	0.700* (0.379)	-0.046** (0.023)	0.010 (0.395)	1.709
$\kappa = 7$	0.350*** (0.097)	0.008 (0.005)	-0.123* (0.071)	0.290 (0.372)	-0.039 (0.024)	0.181 (0.384)	1.606
$\kappa = 8$	0.290*** (0.097)	0.007 (0.005)	-0.109 (0.067)	0.372 (0.354)	-0.034 (0.025)	-0.001 (0.354)	1.231
$\kappa = 9$	0.279*** (0.091)	0.007 (0.005)	-0.119** (0.060)	-0.021 (0.349)	-0.024 (0.027)	0.139 (0.323)	1.058
$\kappa = 10$	0.251*** (0.086)	0.007* (0.004)	-0.114** (0.056)	-0.091 (0.355)	-0.022 (0.025)	0.141 (0.305)	0.918
$\kappa = 11$	0.240*** (0.078)	0.007* (0.004)	-0.108** (0.052)	-0.151 (0.354)	-0.020 (0.022)	0.136 (0.305)	0.973
$\kappa = 12$	0.230*** (0.072)	0.007** (0.003)	-0.104** (0.050)	-0.142 (0.332)	-0.022 (0.019)	0.149 (0.309)	1.001

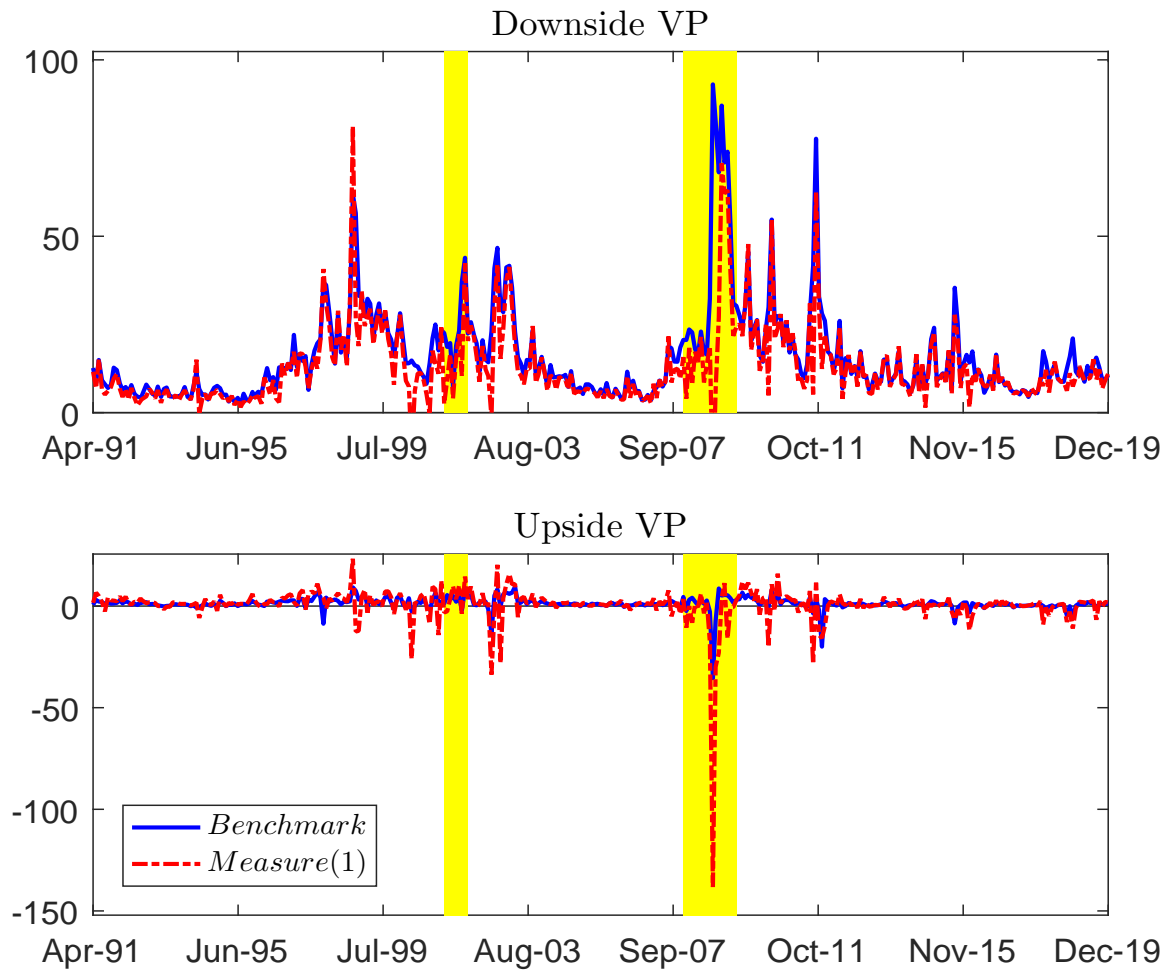


Figure A1: Alternative measures of the VP and its components

The dashed lines denote the Martingale measure, or measure (1) in Tables 1 and 2. The solid lines denote the benchmark VP measures used in the main empirical results (Table 1 and Figure 1). The shaded regions indicate NBER recessions.



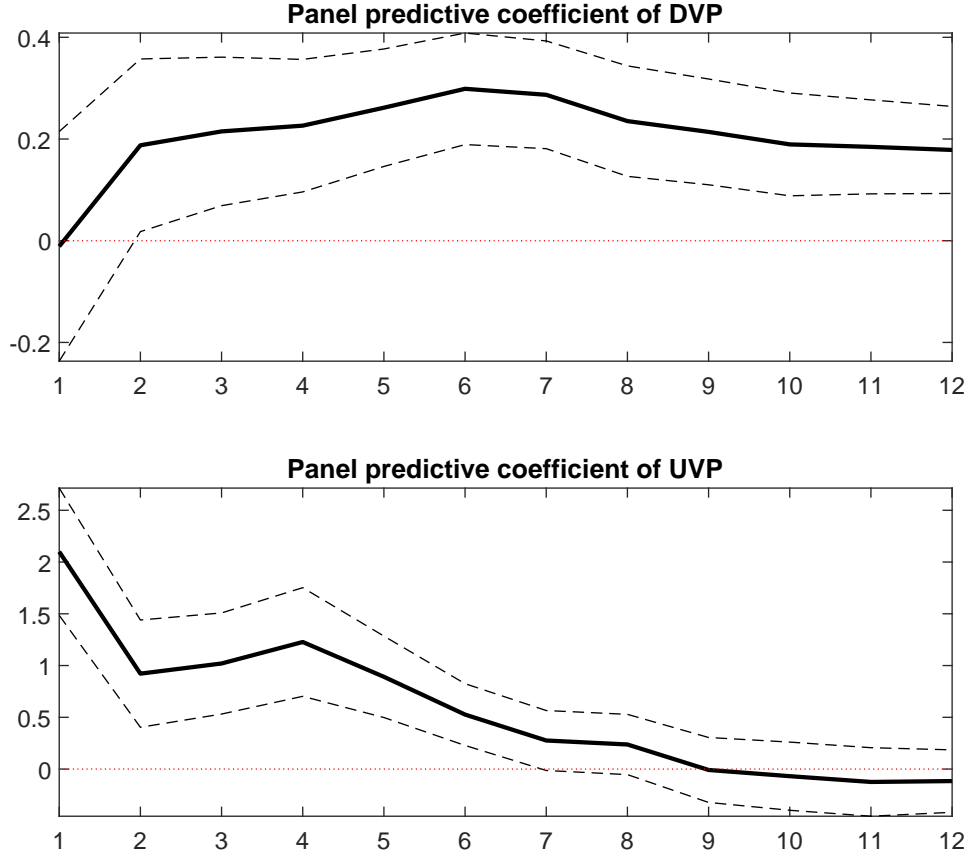


Figure A2: The international stock return predictability of DVP and UVP

This figure shows the predictive coefficient estimates for the downside (DVP, top) and upside (UVP, bottom) variance premiums at horizons between one and 12 months for the main predictability regression setting:

$$\kappa^{-1}r_{i,t,t+\kappa} = a_{i,\kappa} + a_{\kappa} + b_{\kappa}^D vp_{t,t+1}^D + b_{\kappa}^U vp_{t,t+1}^U + \epsilon_{i,t,t+\kappa},$$

where  $r_{i,t,t+\kappa}$  denotes the cumulative  $\kappa$ -month-ahead log excess returns for country  $i$ . The dashed lines depict 90% confidence intervals given Newey-West standard errors.

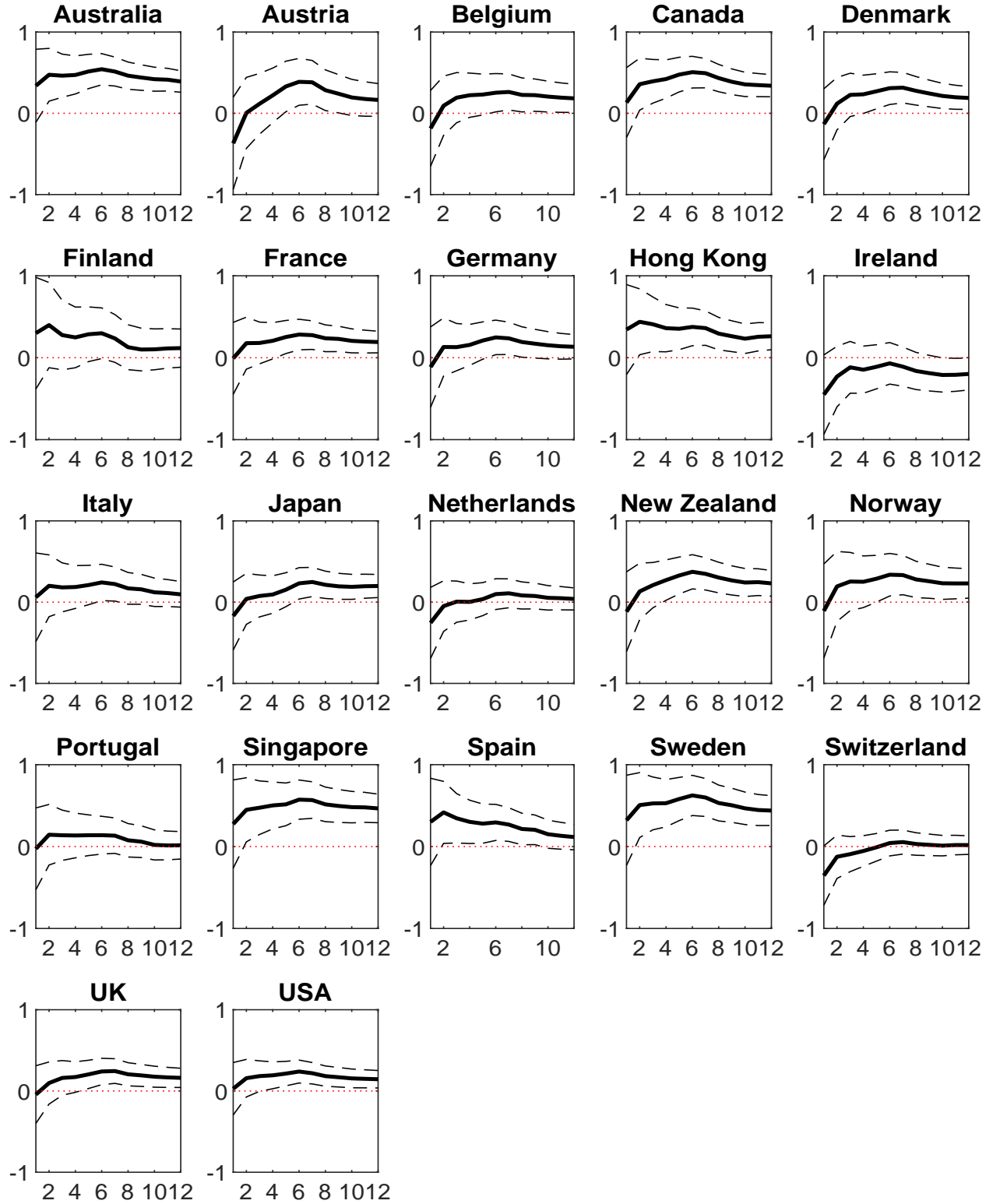


Figure A3: DVP coefficients, country-level regression

This figure shows the predictive coefficient estimates of the downside variance premium (the solid lines) and its 90% confidence interval given Newey-West standard errors (the dashed lines) at the country level. The regression setting is the following:

$$\kappa^{-1}r_{i,t,t+\kappa} = a_{i,\kappa} + b_{i,\kappa}^D vp_{t,t+1}^D + b_{i,\kappa}^U vp_{t,t+1}^U + \epsilon_{i,t,t+\kappa},$$

where  $r_{i,t,t+\kappa}$  denotes the cumulative  $\kappa$ -month-ahead log excess returns for country  $i$ .

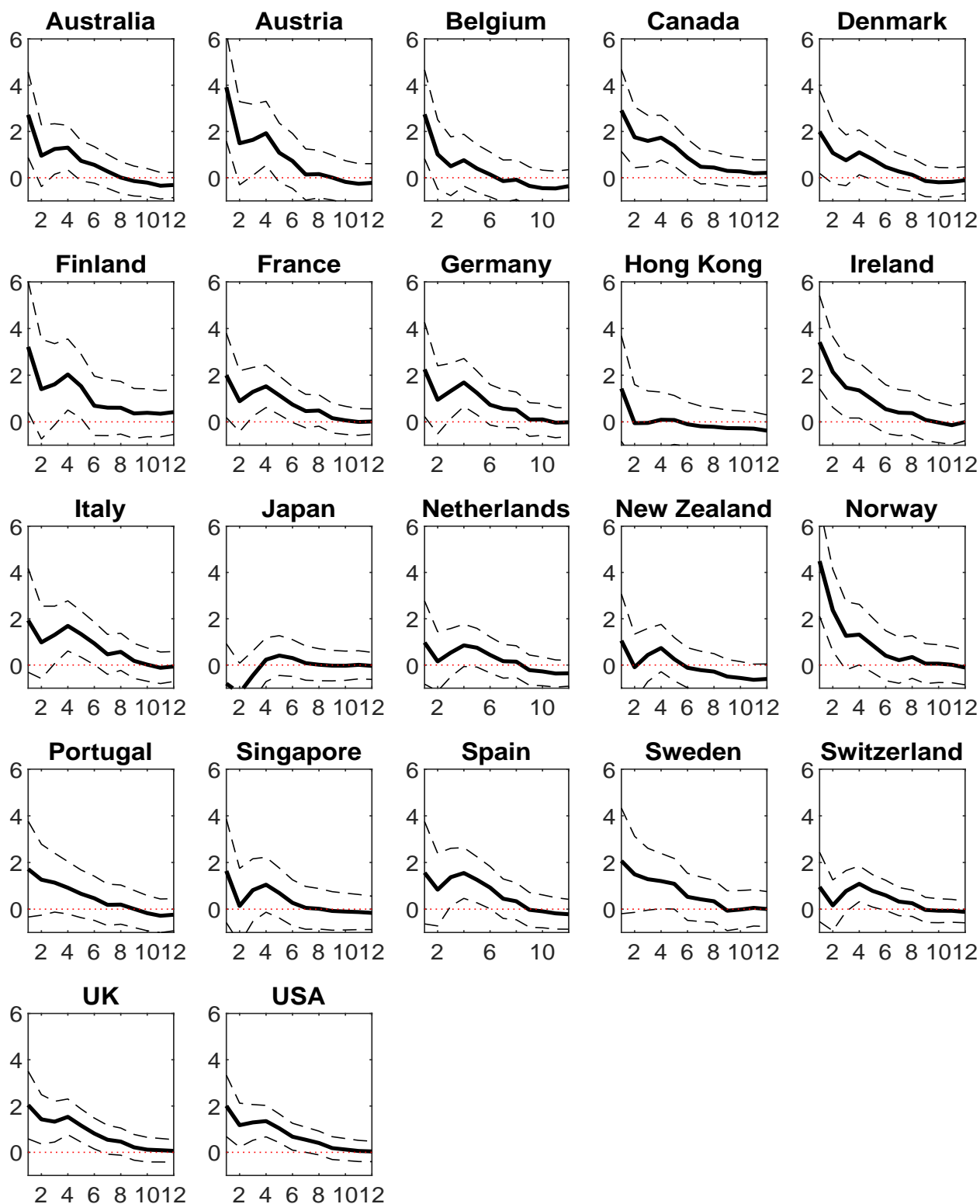


Figure A4: UVP coefficients, country-level regression

This figure shows the predictive coefficient estimates of the upside variance premium (the solid lines) and its 90% confidence interval given Newey-West standard errors (the dashed lines) at the country level. The regression setting is the following:

$$\kappa^{-1}r_{i,t,t+\kappa} = a_{i,\kappa} + b_{i,\kappa}^D vp_{t,t+1}^D + b_{i,\kappa}^U vp_{t,t+1}^U + \epsilon_{i,t,t+\kappa},$$

where  $r_{i,t,t+\kappa}$  denotes the cumulative  $\kappa$ -month-ahead log excess returns for country  $i$ .

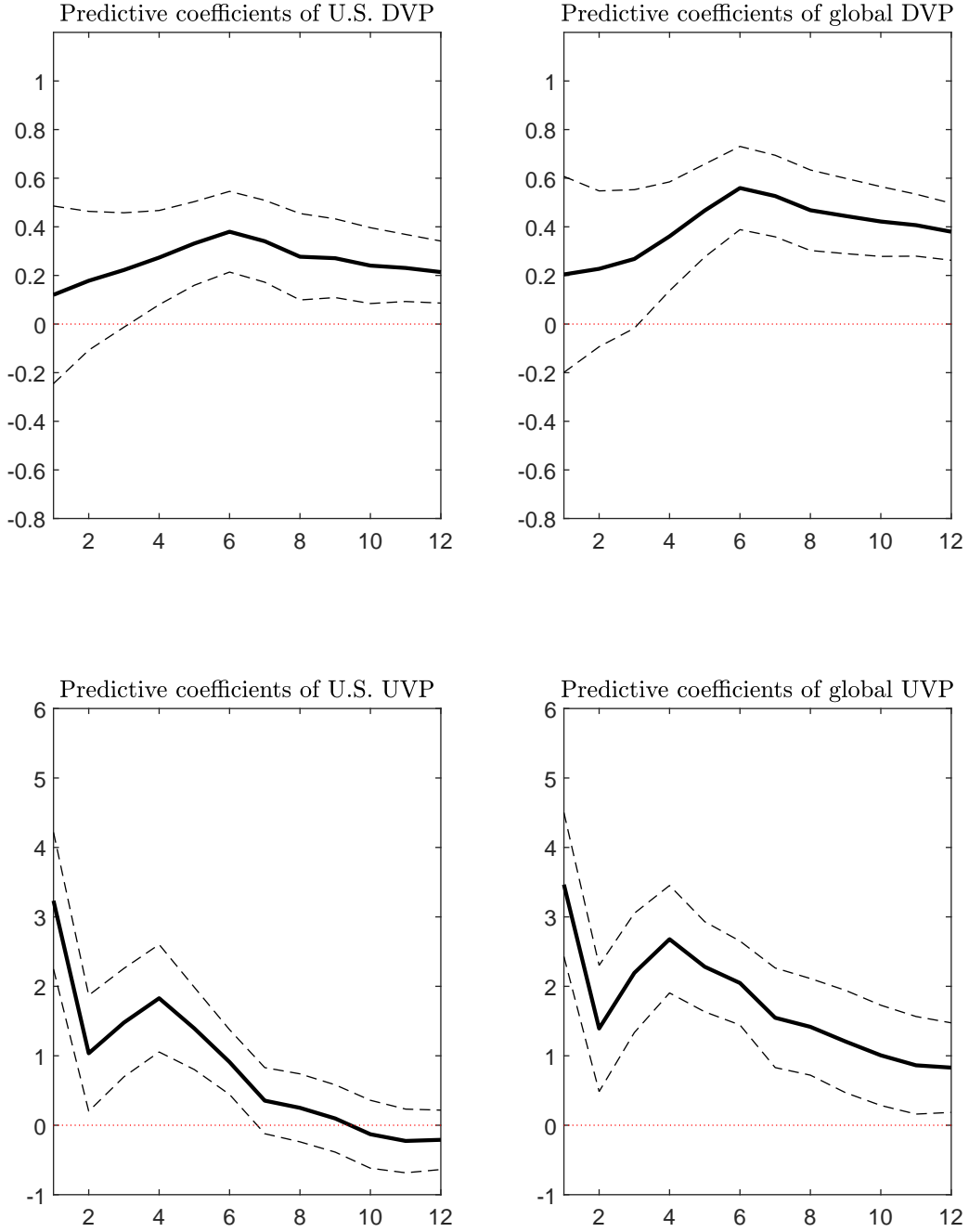


Figure A5: The international stock return predictability of U.S. and global DVP and UVP

This figure shows the predictive coefficient estimates of the downside (DVP, top) and upside (UVP, bottom) variance premiums at horizons between one and 12 months for the main predictability regression setting:

$$\kappa^{-1}r_{i,t,t+\kappa} = a_{\kappa} + b_{\kappa}^D vp_{t,t+1}^D + b_{\kappa}^U vp_{t,t+1}^U + \epsilon_{i,t,t+\kappa},$$

where  $r_{i,t,t+\kappa}$  denotes the cumulative  $\kappa$ -month-ahead log excess returns for country  $i$ . The dashed lines depict 90% confidence intervals given Newey-West standard errors (SEs). The left panels show the coefficients when  $vp^D$  and  $vp^U$  are the variance premium components for the United States, while for the right panels, the variance premium components are the equal-weighted average for the United States, Germany, France, and Switzerland. The sample runs from April 2003 to December 2019. Appendix Page 10

## B. A no-arbitrage international framework

This appendix complements Section 3.1 and solves a simple no-arbitrage international framework to motivate our empirical model. This framework, without loss of generality, consists of a characterization of the state evolution and a pricing kernel for a U.S./global representative agent. The U.S. state evolution process is characterized by kernel state variables, their second-moment state variables, and a cash flow state variable (dividend growth). The dynamic state process,  $\mathbf{Y}_t$ , follows a VAR nature, and the shocks,  $\boldsymbol{\omega}_t$ , are mutually independent centered gamma shocks that introduce heteroskedasticity and non-Gaussianity in an affine state variable system, as follows:

$$\begin{aligned}\mathbf{Y}_{t+1} &= \boldsymbol{\mu} + \mathbf{A}\mathbf{Y}_t + \boldsymbol{\Sigma}\boldsymbol{\omega}_{t+1}, \\ \boldsymbol{\omega}_{t+1} &\sim \Gamma(\boldsymbol{\Omega}\mathbf{Y}_t + \mathbf{e}, \mathbf{1}) - (\boldsymbol{\Omega}\mathbf{Y}_t + \mathbf{e}),\end{aligned}\tag{B1}$$

where  $\boldsymbol{\mu}$ ,  $\mathbf{A}$ ,  $\boldsymbol{\Sigma}$ ,  $\boldsymbol{\Omega}$ , and  $\mathbf{e}$  are constant matrices;  $\Gamma$  represents a gamma distribution;  $\boldsymbol{\Omega}\mathbf{Y}_t + \mathbf{e}$  denotes a vector of shape parameters that spans second (and higher-order) moments of these shocks; and the constant matrix  $\boldsymbol{\Omega}$  describes the relative loadings. The first moment of a gamma distribution  $\Gamma(x, 1)$  is  $x$ , and, therefore,  $\Gamma(\boldsymbol{\Omega}\mathbf{Y}_t + \mathbf{e}, \mathbf{1}) - (\boldsymbol{\Omega}\mathbf{Y}_t + \mathbf{e})$  guarantees that the shocks  $\boldsymbol{\omega}_{t+1}$  follow centered gamma distributions. The loading matrix  $\boldsymbol{\Omega}$  can contain positive, zero, and negative coefficients; this means that a univariate process, such as real growth, can load on multiple shocks on the economy in order to realistically capture their left- and right-tail behaviors. The empirical assumption of asymmetric non-Gaussian shocks allows the framework to be relatively flexible in the estimation while still keeping the model tractable, given their exponential moment-generating functions.

Next, we assume a general linear process of the log U.S. real pricing kernel, as follows:

$$m_{t+1} = m_0 + \mathbf{m}_1\mathbf{Y}_t + \mathbf{m}_2\boldsymbol{\Sigma}\boldsymbol{\omega}_{t+1},\tag{B2}$$

where  $\mathbf{m}_1$  and  $\mathbf{m}_2$  denote the loadings on the lagged state variables and the shocks, respectively.

The U.S./global investor prices individual country dividend growth processes, which load on both global and idiosyncratic kernel and cash flow shocks with heterogeneous degrees of *global exposure*. To be specific, we assume that dividend growth processes for the United States and country  $i$  are, respectively, the following:

$$\Delta d_{t+1} = d_0 + \mathbf{d}_1\mathbf{Y}_t + \mathbf{d}_2\boldsymbol{\Sigma}\boldsymbol{\omega}_{t+1},\tag{B3}$$

$$\Delta d_{t+1}^i = d_0^i + \mathbf{d}_1^i\mathbf{Y}_t + \mathbf{d}_2^i\boldsymbol{\Sigma}\boldsymbol{\omega}_{t+1} + \mu_t^i + u_{d,t+1}^i,\tag{B4}$$

where  $\mathbf{d}_1^i$  ( $\mathbf{d}_2^i$ ) indicates the loadings of country  $i$ 's dividend growth on the U.S. lagged state variable levels (state variable shocks) and  $\mu_t^i$  and  $u_{d,t+1}^i$  indicate, respectively, the additional country-specific dividend growth mean and shock processes that are orthogonal to the U.S. shocks. Both  $\mathbf{d}_1^i$  and  $\mathbf{d}_2^i$  can be motivated to reflect global exposure that can potentially be of an economic or financial nature.

### B.1. Solution: U.S. price-dividend ratio and log returns

Given the no-arbitrage condition, the U.S. price-dividend ratio can be rewritten as,

$$PD_t = E_t \left[ M_{t+1} \left( \frac{P_{t+1} + D_{t+1}}{D_t} \right) \right] = \sum_{n=1}^{\infty} E_t \left[ \exp \left( \sum_{j=1}^n m_{t+j} + \Delta d_{t+j} \right) \right],\tag{B5}$$

where  $m_{t+j}$  indicates the future log U.S. pricing kernel at month  $j$  and  $\Delta d_{t+j}$  the  $j$ -th month log dividend growth rate. Let  $F_t^n$  denote the  $n$ -th term in the summation,  $F_t^n = E_t \left[ \exp \left( \sum_{j=1}^n m_{t+j} + \Delta d_{t+j} \right) \right]$ , and hence  $F_t^n D_t$  is the price of zero-coupon equity that matures in  $n$  periods. The  $PD_t$  can be rewritten as  $\sum_{n=1}^{\infty} F_t^n$ .

We first prove that,  $\forall n \geq 1$ ,  $F_t^n$  is an exactly exponential affine function of the state variables using induction. When  $n = 1$ ,  $F_t^1 = E_t [\exp(m_{t+1} + \Delta d_{t+1})] = E_t \{ \exp[(m_0 + d_0) + (\mathbf{m}_1 + \mathbf{d}_1)\mathbf{Y}_t + (\mathbf{m}_2 + \mathbf{d}_2)\boldsymbol{\Sigma}\boldsymbol{\omega}_{t+1}] \} = \exp(e_0^1 + \mathbf{e}_1^1\mathbf{Y}_t)$ , where  $e_0^1$  and  $\mathbf{e}_1^1$  are implicitly defined. Suppose that the  $(n-1)$ -th term  $F_t^{n-1} =$

$\exp(e_0^{n-1} + e_1^{n-1} Y_t)$ , then

$$\begin{aligned}
F_t^n &= E_t \left[ \exp \left( \sum_{j=1}^n m_{t+j} + \Delta d_{t+j} \right) \right] \\
&= E_t \left\{ \exp(m_{t+1} + \Delta d_{t+1}) \underbrace{E_{t+1} \left[ \exp \left( \sum_{j=1}^{n-1} m_{t+j+1} + \Delta d_{t+j+1} \right) \right]}_{F_{t+1}^{n-1}} \right\} \\
&= E_t \left[ \exp(m_{t+1} + \Delta d_{t+1}) \exp(e_0^{n-1} + e_1^{n-1} Y_{t+1}) \right] = \exp(e_0^n + e_1^n Y_t), \tag{B6}
\end{aligned}$$

where  $e_0^n$  and  $e_1^n$  are implicitly defined. Hence, the price-dividend ratio can be solved as  $PD_t = \sum_{n=1}^{\infty} F_t^n = \sum_{n=1}^{\infty} \exp(e_0^n + e_1^n Y_t)$ . The log return can be solved with linear approximation as

$$\begin{aligned}
r_{t+1} &= \ln \left( \frac{P_{t+1} + D_{t+1}}{P_t} \right) = \Delta d_{t+1} + \ln \left[ \frac{1 + \sum_{n=1}^{\infty} \exp(e_0^n + e_1^n Y_{t+1})}{\sum_{n=1}^{\infty} \exp(e_0^n + e_1^n Y_t)} \right] \\
&\approx \Delta d_{t+1} + \text{const.} + \frac{\sum_{n=1}^{\infty} \exp(e_0^n + e_1^n \bar{Y}) e_1^n}{1 + \sum_{n=1}^{\infty} \exp(e_0^n + e_1^n \bar{Y})} Y_{t+1} - \frac{e_1^n}{\sum_{n=1}^{\infty} \exp(e_0^n + e_1^n \bar{Y})} Y_t \\
&= \xi_0 + \xi_1 Y_t + \xi_2 \Sigma \omega_{t+1}. \tag{B7}
\end{aligned}$$

This produces a linear return process.

## B.2. Solution: International price-dividend ratio and log returns

The model takes the perspective of a U.S. investor. She prices country  $i$ 's cash flow processes in dollars at the equilibrium. Given the common pricing kernel  $m_{t+1}$ , the price-dividend ratio of country  $i$  is modeled as  $PD_t^i = E_t \left[ M_{t+1} \left( \frac{P_{t+1}^i + D_{t+1}^i}{D_t^i} \right) \right] = \sum_{n=1}^{\infty} E_t \left[ \exp \left( \sum_{j=1}^n m_{t+j} + \Delta d_{t+j}^i \right) \right]$ . Using similar induction procedures, it can be shown that

$$PD_t^i = \sum_{n=1}^{\infty} F_t^n = \sum_{n=1}^{\infty} \exp \left( e_0^{i,n} + e_1^{i,n} Y_t + \underbrace{e_2^{i,n} Y_t^i}_{\text{Idiosyncratic Part}} \right), \tag{B8}$$

where  $Y_t^i$  denotes a vector of country-specific state variables. The country  $i$  log market return can be solved and approximated as,

$$\begin{aligned}
r_{t+1}^i &= \ln \left( \frac{P_{t+1}^i + D_{t+1}^i}{P_t^i} \right) = \Delta d_{t+1}^i + \ln \left[ \frac{1 + \sum_{n=1}^{\infty} \exp(e_0^{i,n} + e_1^{i,n} Y_{t+1} + e_2^{i,n} Y_{t+1}^i)}{\sum_{n=1}^{\infty} \exp(e_0^{i,n} + e_1^{i,n} Y_t + e_2^{i,n} Y_t^i)} \right] \\
&\approx \Delta d_{t+1}^i + \text{const.} + \underbrace{\frac{\sum_{n=1}^{\infty} \exp(e_0^{i,n} + e_1^{i,n} \bar{Y} + e_2^{i,n} \bar{Y}^i) e_1^{i,n}}{1 + \sum_{n=1}^{\infty} \exp(e_0^{i,n} + e_1^{i,n} \bar{Y} + e_2^{i,n} \bar{Y}^i)} Y_{t+1} - \frac{e_1^{i,n}}{\sum_{n=1}^{\infty} \exp(e_0^{i,n} + e_1^{i,n} \bar{Y} + e_2^{i,n} \bar{Y}^i)} Y_t}_{\text{Global exposure}} \\
&\quad + \underbrace{\frac{\sum_{n=1}^{\infty} \exp(e_0^{i,n} + e_1^{i,n} \bar{Y} + e_2^{i,n} \bar{Y}^i) e_2^{i,n}}{1 + \sum_{n=1}^{\infty} \exp(e_0^{i,n} + e_1^{i,n} \bar{Y} + e_2^{i,n} \bar{Y}^i)} Y_{t+1}^i - \frac{e_2^{i,n}}{\sum_{n=1}^{\infty} \exp(e_0^{i,n} + e_1^{i,n} \bar{Y} + e_2^{i,n} \bar{Y}^i)} Y_t^i}_{\text{Idiosyncratic}} \\
&= \xi_0^i + \xi_1^i Y_t + \xi_2^i \Sigma \omega_{t+1} + \text{Idiosyncratic Parts.} \tag{B9}
\end{aligned}$$

In this framework, international stock returns are differentiated through cash flow capitalizations, where country cash flow growths are assumed with different levels of exposure to various global shocks. Intuitively,  $\xi_2^i$  is crucial in determining country  $i$ 's risk premiums. Two sources of cross-country heterogeneity in  $\xi_2^i$  can be shown in a closed-form model solution, one through the pure cash flow growth  $\Delta d_{t+1}^i$  and another through the changes in country  $i$ 's log price-dividend ratio. First, we explicitly assume that country  $i$ 's cash flow growth loads on global shocks through  $d_2^i$ . Second, when global economic uncertainty increases, country  $i$ 's future dividend growth (i.e., modeled as  $d_1^i$ ) is expected to decrease, driving down the current stock price. A bad global economic or risk aversion shock could also induce different intertemporal substitution or precautionary savings effects for different countries due to varying exposure of dividend growth to global shocks (i.e., modeled as  $d_2^i$ ), changing the interest rates and hence the total return demanded in an individual country. Therefore, both  $d_1^i$  and  $d_2^i$  can enter country  $i$ 's price-dividend ratio, and both can motivate heterogeneity of  $\xi_2^i$  in  $r_{t+1}^i$ .

### B.3. Solution: Variance risk premium

We derive U.S. one-period conditional stock return variances under the physical and risk-neutral expectations. First, the U.S. one-period physical conditional return variance can be easily obtained, given that  $\omega_{t+1} \sim \Gamma(\Omega Y_t + e, 1) - (\Omega Y_t + e)$ , as

$$VAR_t(r_{t+1}) = (\xi_2 \Sigma)^{\circ 2} (\Omega Y_t + e), \quad (\text{B10})$$

where “ $\circ$ ” indicates element-by-element matrix multiplication.

Second, the U.S. one-period risk-neutral conditional return variance can be obtained using the moment generating function (MGF) of gamma-distributed shocks. We start from the MGF under the risk-neutral measure

$$\begin{aligned} mgf_t^Q(r_{t+1}; \nu) &= \frac{E_t[\exp(m_{t+1} + \nu r_{t+1})]}{E_t[\exp(m_{t+1})]} \\ &= \exp\{E_t(m_{t+1}) + \nu E_t(r_{t+1}) + [-(\mathbf{m}_2 + \nu \xi_2) \Sigma - \ln(1 - (\mathbf{m}_2 + \nu \xi_2) \Sigma)] (\Omega Y_t + e)\} \\ &\quad / \exp\{E_t(m_{t+1}) + [-\mathbf{m}_2 \Sigma - \ln(1 - \mathbf{m}_2 \Sigma)] (\Omega Y_t + e)\} \\ &= \exp\{\nu E_t(r_{t+1}) + [-\nu \xi_2 \Sigma + [-\ln(1 - (\mathbf{m}_2 + \nu \xi_2) \Sigma) + \ln(1 - \mathbf{m}_2 \Sigma)]] (\Omega Y_t + e)\}. \end{aligned}$$

The first-order moment is the first-order derivative at  $\nu = 0$ ,

$$\begin{aligned} \frac{\partial mgf_t^Q(r_{t+1}; \nu)}{\partial \nu} &= mgf_t^Q(r_{t+1}; \nu) * \left\{ E_t(r_{t+1}) + [(\mathbf{m}_2 + \nu \xi_2) \Sigma \circ \xi_2 \Sigma \circ (1 - (\mathbf{m}_2 + \nu \xi_2) \Sigma)^{\circ -1}] (\Omega Y_t + e) \right\} \\ E_t^Q(r_{t+1}) &= \frac{\partial mgf_t^Q(r_{t+1}; \nu)}{\partial \nu} \Big|_{\nu=0} \\ &= E_t(r_{t+1}) + [\mathbf{m}_2 \Sigma \circ \xi_2 \Sigma \circ (1 - \mathbf{m}_2 \Sigma)^{\circ -1}] (\Omega Y_t + e). \end{aligned}$$

The second-order moment can be derived as follows:

$$\begin{aligned} \frac{\partial^2 mgf_t^Q(r_{t+1}; \nu)}{\partial \nu^2} &= mgf_t^Q(r_{t+1}; \nu) * \left\{ E_t(r_{t+1}) + [(\mathbf{m}_2 + \nu \xi_2) \Sigma \circ \xi_2 \Sigma \circ (1 - (\mathbf{m}_2 + \nu \xi_2) \Sigma)^{\circ -1}] (\Omega Y_t + e) \right\}^2 \\ &\quad + mgf_t^Q(r_{t+1}; \nu) * \left\{ [(\mathbf{m}_2 + \nu \xi_2) \Sigma \circ (\xi_2 \Sigma)^{\circ 2} - (1 - (\mathbf{m}_2 + \nu \xi_2) \Sigma) \circ (\xi_2 \Sigma)^{\circ 2}] \circ (1 - (\mathbf{m}_2 + \nu \xi_2) \Sigma) \right\} \\ E_t^Q(r_{t+1}^2) &= \frac{\partial^2 mgf_t^Q(r_{t+1}; \nu)}{\partial \nu^2} \Big|_{\nu=0} \\ &= \left( E_t^Q(r_{t+1}) \right)^2 + [(\xi_2 \Sigma)^{\circ 2} \circ (1 - \mathbf{m}_2 \Sigma)^{\circ -2}] (\Omega Y_t + e). \end{aligned}$$

As a result, the one-period risk-neutral conditional variance is

$$\begin{aligned} VAR_t^Q(\tilde{r}_{t+1}^i) &= E_t^Q((\tilde{r}_{t+1}^i)^2) - \left( E_t^Q(\tilde{r}_{t+1}^i) \right)^2 \\ &= [(\xi_2 \Sigma)^{\circ 2} \circ (1 - \mathbf{m}_2 \Sigma)^{\circ -2}] (\Omega Y_t + e). \end{aligned}$$

The U.S. variance risk premium,  $VAR_t^Q(\tilde{r}_{t+1}^i) - VAR_t(\tilde{r}_{t+1}^i)$ , is hence given by:

$$VAR_t^Q(\tilde{r}_{t+1}^i) - VAR_t(\tilde{r}_{t+1}^i) = \left\{ (\boldsymbol{\xi}_2 \boldsymbol{\Sigma})^{\circ 2} \circ \left[ (\mathbf{1} - \mathbf{m}_2 \boldsymbol{\Sigma})^{\circ -2} - \mathbf{1} \right] \right\} (\boldsymbol{\Omega} \mathbf{Y}_t + \mathbf{e}), \quad (\text{B11})$$

where “ $\circ$ ” denotes element-by-element matrix multiplication.

This provides some economic insights. First, the dynamics of VP (and its downside and upside components) should be driven by the shape parameters of kernel state variable shocks, here specified as  $\boldsymbol{\Omega} \mathbf{Y}_t + \mathbf{e}$ . This is because, for these shocks, the pricing kernel has non-zero loadings (that is,  $m_2 \neq 0$ ). Second, for shocks with positive  $m_2$  loadings, their shape parameters (as captured in  $(\boldsymbol{\Omega} \mathbf{Y}_t + \mathbf{e})$ ) contribute positively to VP, given  $\left[ \left( \frac{1}{1 - m_2 \sigma} \right)^2 - 1 \right] > 0$ . Intuitively, for instance, in a standard habit formation model, the marginal utility loads positively on relative risk aversion, and, hence, VP in such a framework would increase with the expected variability in risk aversion; in the long-run risk model of Segal, Shaliastovich, and Yaron (2015), the kernel has a positive exposure to a bad macroeconomic shock, and, hence, VP could also increase with bad macroeconomic uncertainty.

Note that it is not trivial to derive model-implied VP components that are consistent with the downside and upside definitions as in our empirical section (negative and positive return realizations, respectively, in Section 2) because returns are endogenously determined, as shown in Equation (B7). Therefore, given the empirical focus of the paper, we choose to determine and separate the drivers of downside and upside VPs entirely empirically and let the data speak, as discussed in Section 3.1. Such an empirical approach is motivated from what we learn in this appendix section: that VP should be spanned by second moments of kernel shocks and so should its components.

## B.4. Solution: Equity risk premiums

The risk-free rate is derived as

$$\begin{aligned} rf_t &= -\ln \{E_t[\exp(m_{t+1})]\} \\ &= -\ln \{E_t(m_{t+1}) + [-\mathbf{m}_2 \boldsymbol{\Sigma} - \ln(\mathbf{1} - \mathbf{m}_2 \boldsymbol{\Sigma})](\boldsymbol{\Omega} \mathbf{Y}_t + \mathbf{e})\}. \end{aligned} \quad (\text{B12})$$

We then impose the no-arbitrage condition,  $1 = E_t[\exp(m_{t+1} + r_{t+1})]$  and obtain the expected excess returns. By expanding the law of one price equation, we obtain

$$\begin{aligned} 1 &= E_t[\exp(m_{t+1} + r_{t+1})] \\ &= \exp \{E_t(m_{t+1}) + E_t(r_{t+1}) + [-(\mathbf{m}_2 + \boldsymbol{\xi}_2) \boldsymbol{\Sigma} - \ln(\mathbf{1} - (\mathbf{m}_2 + \boldsymbol{\xi}_2) \boldsymbol{\Sigma})](\boldsymbol{\Omega} \mathbf{Y}_t + \mathbf{e})\}, \end{aligned}$$

where  $\mathbf{m}_2$ ,  $\boldsymbol{\xi}_2$ ,  $\boldsymbol{\Sigma}$ , and  $\mathbf{e}$  are constant matrices defined above. Given the risk free rate derived above, the U.S. equity risk premium is given by:

$$E_t(r_{t+1}) - rf_t = \{\boldsymbol{\xi}_2 \boldsymbol{\Sigma} + \ln[\mathbf{1} - (\mathbf{m}_2 + \boldsymbol{\xi}_2) \boldsymbol{\Sigma}] - \ln(\mathbf{1} - \mathbf{m}_2 \boldsymbol{\Sigma})\} (\boldsymbol{\Omega} \mathbf{Y}_t + \mathbf{e}), \quad (\text{B13})$$

which is determined by second moments of shocks that commonly drive the pricing kernel and asset returns. Similarly, these U.S. second moments also determine the global compensation part of country  $i$ 's one-month-ahead equity risk premium ( $EP_{1,t}^i$ ) in our framework, as follows:

$$\begin{aligned} E_t(r_{t+1}^i) - rf_t &= \underbrace{\{\boldsymbol{\xi}_2^i \boldsymbol{\Sigma} + \ln[\mathbf{1} - (\mathbf{m}_2 + \boldsymbol{\xi}_2^i) \boldsymbol{\Sigma}] - \ln(\mathbf{1} - \mathbf{m}_2 \boldsymbol{\Sigma})\}}_{\text{The Global Compensation Part}} (\boldsymbol{\Omega} \mathbf{Y}_t + \mathbf{e}) \\ &\quad + \text{Idiosyncratic Parts.} \end{aligned} \quad (\text{B14})$$

The Gaussian approximation of the US return equation above is  $-(\mathbf{m}_2 \boldsymbol{\Sigma} \circ \boldsymbol{\xi}_2 \boldsymbol{\Sigma})(\boldsymbol{\Omega} \mathbf{Y}_t + \mathbf{e})$ , or  $-Cov_t(r_{t+1}, m_{t+1})$ ; similarly, for other countries, the global part captures  $-Cov_t(r_{t+1}^i, m_{t+1})$ . The total country equity risk premiums can also be driven by a pure local risk compensation component, which, however, is not the focus of the paper and in theory should be unpredictable by common/U.S. predictors, and, hence, is abbreviated above without loss of generality.

In summary, this framework suggests two important implications for our research objective. First, both the dynamics of VP and the global part of international EPs should be driven by the second moments of kernel shocks. Second, this commonality implies various stock return predictability channels, which



together relate to the observed international predictive coefficients.

## C. Additional empirical evidence for Sections 3.2 and 5

### C.1. Dynamic processes

We present precise processes to estimate the equation system (12). The economic growth state variable is assumed to follow a reduced-form dynamic process that captures time-varying expected growth and asymmetric/skewed and heteroskedastic shocks to be potentially consistent with recent work (see, e.g., Adrian, Boyarchenko, and Giannone (2019)):

$$\theta_{t+1} = \bar{\theta} + \rho_{\theta,\theta}(\theta_t - \bar{\theta}) + \rho_{\theta,\theta_p}(\theta_p t - \bar{\theta_p}) + \rho_{\theta,\theta_n}(\theta_n t - \bar{\theta_n}) + \delta_{\theta,\theta_p}\omega_{\theta_p,t+1} - \delta_{\theta,\theta_n}\omega_{\theta_n,t+1}, \quad (\text{C15})$$

where the conditional mean is subject to an AR(1) term capturing persistence as well as changes in expected good and bad economic uncertainties capturing the GARCH-in-mean intuition. As in Bekaert, Engstrom, and Xu (2022), the disturbance of the log economic growth is decomposed into two independent centered gamma shocks, as follows:

$$\begin{aligned} \omega_{\theta_p,t+1} &= \Gamma(\theta_p t, 1) - \theta_p t, \\ \omega_{\theta_n,t+1} &= \Gamma(\theta_n t, 1) - \theta_n t, \end{aligned}$$

where  $\omega_{\theta_p,t+1}$  ( $\omega_{\theta_n,t+1}$ ) governs the right-tail (left-tail) dynamics of the growth distribution with shape parameter  $\theta_p t$  ( $\theta_n t$ ) determining the conditional higher moments of the growth disturbance shock. For example, given the moment generating function (MGF) of independent gamma shocks, the conditional variance of  $\theta_{t+1}$  is  $\delta_{\theta,\theta_p}^2 \theta_p t + \delta_{\theta,\theta_n}^2 \theta_n t$  and the conditional unscaled skewness is  $2\delta_{\theta,\theta_p}^3 \theta_p t - 2\delta_{\theta,\theta_n}^3 \theta_n t$ . Increases in  $\theta_p t$  ( $\theta_n t$ ) imply higher (lower) conditional skewness while increasing conditional variance, and, hence,  $\theta_p t$  ( $\theta_n t$ ), can be interpreted as the “good” (“bad”) uncertainty state variable. This disturbance structure is one of the non-Gaussian shock assumptions that the literature has explored to realistically model macro or financial state variable processes (see, e.g., Eraker and Shaliastovich (2008); Fulop, Li, and Yu (2015); Segal, Shaliastovich, and Yaron (2015); De Groot (2015); Bekaert and Engstrom (2017); and Xu (2021)). The dynamics of the good and bad economic uncertainty state variables follow AR(1) processes:

$$\theta_p t_{t+1} = \bar{\theta_p} + \rho_{\theta_p}(\theta_p t - \bar{\theta_p}) + \sigma_{\theta_p}\omega_{\theta_p,t+1}, \quad (\text{C16})$$

$$\theta_n t_{t+1} = \bar{\theta_n} + \rho_{\theta_n}(\theta_n t - \bar{\theta_n}) + \sigma_{\theta_n}\omega_{\theta_n,t+1}. \quad (\text{C17})$$

We define a macroeconomic state variable vector,  $\mathbf{Y}_{\text{mac},t} \equiv [\theta_t \ \theta_p t \ \theta_n t]'$ , and its unconditional mean  $\overline{\mathbf{Y}_{\text{mac}}} \equiv [\bar{\theta} \ \bar{\theta_p} \ \bar{\theta_n}]'$ . The risk aversion state variable,  $q_t$ , evolves over time with a state-dependent conditional mean and a disturbance that is exposed to fundamental economic shocks. The residual is then separated into two independent gamma shocks,  $\omega_{q_h,t+1}$  and  $\omega_{q_l,t+1}$ , potentially capturing distinct behaviors of the right-tail (high risk aversion) and left-tail (low risk aversion) preference shocks:

$$\begin{aligned} q_{t+1} &= \bar{q} + \rho_{q,q}(q_t - \bar{q}) + \rho_{q,q_h}(q_h t - \bar{q_h}) + \rho_{q,\text{mac}}(\mathbf{Y}_{\text{mac},t} - \overline{\mathbf{Y}_{\text{mac}}}) \\ &\quad + \delta_{q,\theta_p}\omega_{\theta_p,t+1} + \delta_{q,\theta_n}\omega_{\theta_n,t+1} + \delta_{q,q_h}\omega_{q_h,t+1} - \delta_{q,q_l}\omega_{q_l,t+1}, \\ \omega_{q_h,t+1} &= \Gamma(q_h t, 1) - q_h t, \\ \omega_{q_l,t+1} &= \Gamma(\bar{q_l}, 1) - \bar{q_l}, \\ q_h t_{t+1} &= \bar{q_h} + \rho_{q_h}(q_h t - \bar{q_h}) + \sigma_{q_h}\omega_{q_h,t+1}. \end{aligned} \quad (\text{C18})$$

The conditional mean of risk aversion evolves with the macro variables (both level and volatility), an AR(1) term, and a high risk aversion state variable  $q_h t$  that captures the fluctuation of the right-tail risk aversion shock. Given that risk aversion heteroskedasticity is likely driven by its right-tail movements when risk aversion is high, we shut down heteroskedasticity coming from the left-tail movements when risk aversion is low to keep the model relatively simple. Note that our risk aversion dynamics are different from those in the literature. First, Bekaert, Engstrom, and Xu (2022) also assume a pure risk aversion shock that is orthogonal to consumption (fundamental) shocks; they assume its shape parameter is the

same as risk aversion, whereas we elicit a new state variable  $qh_t$  that does not equal  $q_t$  (but should very likely positively correlate with  $q_t$  empirically, as we do find later). Second, the most acknowledged time-varying risk aversion model is Campbell and Cochrane (1999), which assumes that risk aversion is purely driven by changes in real fundamentals. Finally, we set  $\mathbf{Y}_{q,t} = [q_t \ qh_t]'$ , and  $\overline{\mathbf{Y}}_q = [\bar{q} \ \overline{qh}]'$ .

## C.2. Estimation results

The estimation of the three state variable system is conducted sequentially given the overlaying shocks. First, the economic growth and uncertainty state variables are estimated using a monthly sample from 1947/02 to 2019/12 and the Approximate Maximum Likelihood (AML) methodology in Bates (2006). Then, the risk aversion measure uses the  $q_t$  series from Bekaert, Engstrom, and Xu (2022), covering from 1986/06 to 2019/12, and is first projected on known macro variables; the disturbance is estimated following Bates (2006). Below are the estimation results (\*\*\*) (\*\*, \*): 1% (5%, 10%) test):

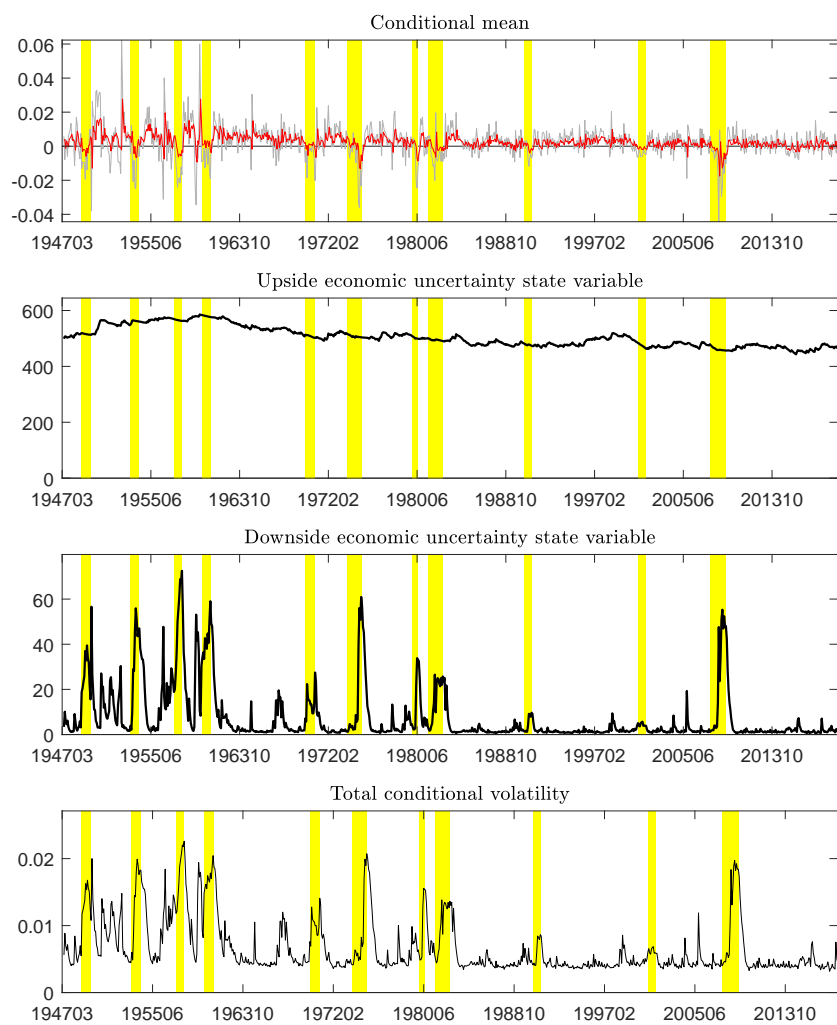
A. Estimation Results of $\theta_t, \theta p_t, \theta n_t$						
$\theta_t$ :	$\bar{\theta}$	$\rho_{\theta,\theta}$	$\rho_{\theta,\theta p}$	$\rho_{\theta,\theta n}$	$\delta_{\theta,\theta p}$	$\delta_{\theta,\theta n}$
Coeff.	0.0023***	0.3799***	4.02E-05	-0.0001	0.0001***	0.0028***
SE	(0.0003)	(0.0313)	(0.0002)	(0.0012)	(2.81E-5)	(0.0003)
$\theta p_t$ :	$\bar{\theta p}$	$\rho_{\theta p}$	$\delta_{\theta p}$			
Coeff.	500 (fix)	0.9979***	0.3739***			
SE		(0.0171)	(0.0173)			
$\theta n_t$ :	$\bar{\theta n}$	$\rho_{\theta n}$	$\delta_{\theta p}$			
Coeff.	10.3362***	0.9525***	2.2996***			
SE	(2.0747)	(0.0096)	(0.1907)			
B. Estimation Results of $q_t, qh_t$						
$q_t$ :	$\bar{q}$	$\rho_{q,q}$	$\rho_{q,qh}$	$\rho_{q,\theta}$	$\rho_{q,\theta p}$	$\rho_{q,\theta n}$
Coeff.	0.3266***	0.7124***	-0.0006	-3.1851***	0.0008**	0.0011
SE	(0.0102)	(0.0355)	(0.0004)	(0.9238)	(0.0003)	(0.0009)
	$\delta_{q,\theta p}$	$\delta_{q,\theta n}$	$\delta_{q,qh}$	$\delta_{q,ql}$	$\overline{ql}$	
Coeff.	0.0004	0.0185***	1.0767***	0.0906***	786.6892***	
SE	(0.0003)	(0.0034)	(0.0645)	(0.0001)	(102.74)	
$qh_t$ :	$\overline{qh}$	$\rho_{qh}$	$\delta_{qh}$			
Coeff.	0.872***	0.5677***	1.0767***			
SE	(0.0670)	(0.0307)	(0.0645)			

We next compare the closeness between average conditional moments (mean, variance) and empirical unconditional moments of  $\theta_{t+1}$  and  $q_{t+1}$ . Moment matching is expected because of the highly specified model assumptions; given that our paper is not about selecting the most efficient dynamic process but obtaining realistic estimates of state variables, we do not expand the model comparison exercise and follow existing evidence and frameworks in the literature.

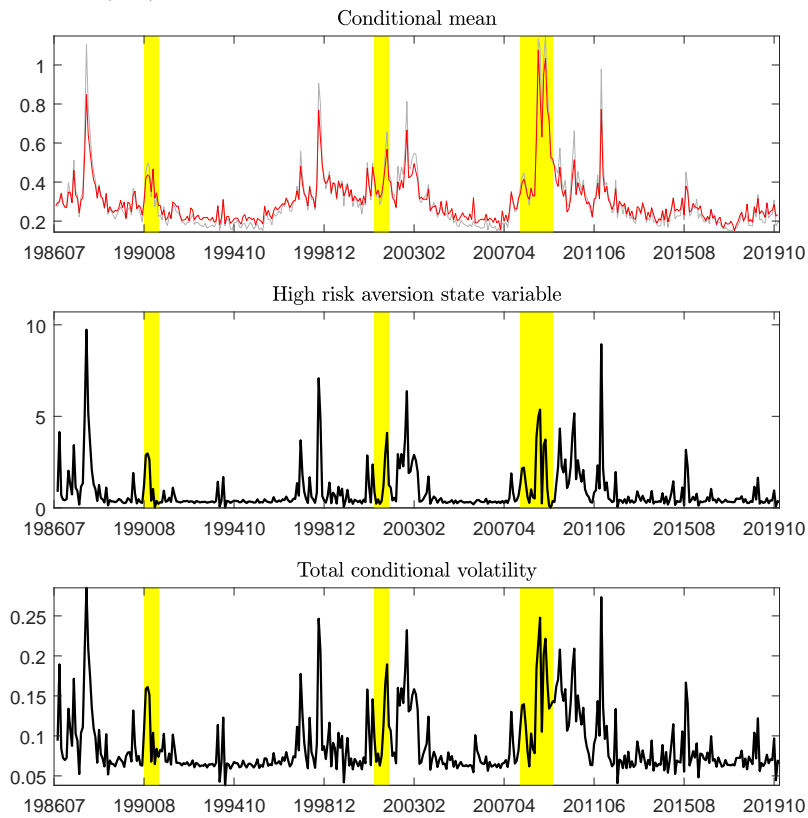
	$\theta_{t+1}$		$q_{t+1}$	
	Data	Model	Data	Model
Mean	0.0023*** (0.0003)	<b>0.0025</b>	0.3023*** (0.0084)	<b>0.3049</b>
Variance	7.33E-05*** (7.73E-06)	<b>6.11E-05</b>	0.0091*** (0.0018)	<b>0.0094</b>

The figures below depict the dynamics of state variables in the macro and risk aversion, respectively:

- (1) From top to bottom: Economic growth (gray) and its conditional mean (red); good macro uncertainty state variable  $\theta p_t$ ; bad macro uncertainty state variable  $\theta n_t$ ; total conditional volatility.



(2) From top to bottom: Risk aversion state variable  $q_t$  from Bekaert, Engstrom, and Xu (2022) (gray) and its conditional mean (red); high risk aversion state variable  $qh_t$ ; total conditional volatility.



### C.3. Variance decomposition of international equity risk premiums: A cross-country view

This figure complements Figure 4-(B) with a cross-country view and Figure 6 with a variance decomposition perspective. This plot shows the variance decomposition (in %) of the model-implied international equity risk premiums at various horizons coming from different sources of state variables; by construction, at each horizon, the sum of the three numbers adds to 100%. The results are calibrated using low/high economic and financial exposure, with low (high) being below the 33th (above the 67th) percentile value of the 22 countries; see construction and data details in Table 4.

